

# Vertical profiles of O<sub>3</sub> and NO<sub>x</sub> chemistry in the polluted nocturnal boundary layer in Phoenix, AZ: I. Field observations by long-path DOAS

S. Wang, R. Ackermann, and J. Stutz

Department of Atmospheric and Oceanic Sciences, University of California, Los Angeles, CA, USA

Received: 18 October 2005 – Published in Atmos. Chem. Phys. Discuss.: 3 January 2006

Revised: 4 April 2006 – Accepted: 29 May 2006 – Published: 6 July 2006

**Abstract.** Nocturnal chemistry in the atmospheric boundary layer plays a key role in determining the initial chemical conditions for photochemistry during the following morning as well as influencing the budgets of O<sub>3</sub> and NO<sub>2</sub>. Despite its importance, chemistry in the nocturnal boundary layer (NBL), especially in heavily polluted urban areas, has received little attention so far, which greatly limits the current understanding of the processes involved. In particular, the influence of vertical mixing on chemical processes gives rise to complex vertical profiles of various reactive trace gases and makes nocturnal chemistry altitude-dependent. The processing of pollutants is thus driven by a complicated, and not well quantified, interplay between chemistry and vertical mixing.

In order to gain a better understanding of the altitude-dependent nocturnal chemistry in the polluted urban environment, a field study was carried out in the downtown area of Phoenix, AZ, in summer 2001. Vertical profiles of reactive species, such as O<sub>3</sub>, NO<sub>2</sub>, and NO<sub>3</sub>, were observed in the lowest 140 m of the troposphere throughout the night. The disappearance of these trace gas vertical gradients during the morning coincided with the morning transition from a stable NBL to a well-mixed convective layer. The vertical gradients of trace gas levels were found to be dependent on both surface NO<sub>x</sub> emission strength and the vertical stability of the NBL. The vertical gradients of O<sub>x</sub>, the sum of O<sub>3</sub> and NO<sub>2</sub>, were found to be much smaller than those of O<sub>3</sub> and NO<sub>2</sub>, revealing the dominant role of NO emissions followed by the O<sub>3</sub>+NO reaction for the altitude-dependence of nocturnal chemistry in urban areas. Dry deposition, direct emissions, and other chemical production pathways of NO<sub>2</sub> also play a role for the O<sub>x</sub> distribution. Strong positive vertical gradients of NO<sub>3</sub>, that are predominantly determined by NO<sub>3</sub> loss near the ground, were observed. The vertical profiles of NO<sub>3</sub> and the calculated vertical profiles of its reser-

voir species (N<sub>2</sub>O<sub>5</sub>) confirm earlier model results suggesting complex vertical distributions of atmospheric denoxification processes during the night.

## 1 Introduction

Nocturnal chemistry in the polluted urban boundary layer has received surprisingly little attention thus far, despite its significance in determining initial conditions for photochemistry during the following day. It is well known that daytime chemistry is driven by photolytic reactions involving nitrogen oxides (NO<sub>x</sub>), hydrocarbons, and hydroxyl radicals (HO<sub>x</sub>) that lead to the formation of O<sub>3</sub> and particles. In contrast, at night O<sub>3</sub> undergoes a net loss in the absence of sunlight through dry deposition, NO titration, and other chemical pathways. The difference in O<sub>3</sub> chemistry between day and night leads to a diurnal cycle of high daytime and low night-time O<sub>3</sub> levels in the boundary layer in both rural and urban areas (Aneja et al., 2000; Colbeck and Harrison, 1985; Van Dop et al., 1977). While OH chemistry becomes less important during night-time (Abram et al., 2000; Alicke et al., 2002; Smith et al., 2002), the nitrate radical (NO<sub>3</sub>) as well as O<sub>3</sub> become the dominant oxidants determining the budget of NO<sub>x</sub> and VOCs (Geyer, 2000; Jenkin and Clemitshaw, 2000; Sadanaga et al., 2003). In addition, nocturnal chemistry also influences the aerosol composition, for example, through the uptake of the NO<sub>3</sub> reservoir species, N<sub>2</sub>O<sub>5</sub> (Dentener and Crutzen, 1993; Geyer, 2000).

The absence of solar radiation at night also leads to radiative cooling of the surface which inhibits turbulence and vertical mixing. As a result, a stable nocturnal boundary layer (NBL), which is capped by a relatively well-mixed residual layer (RL) with neutral stability, develops. Due to the weak vertical mixing, ground-level emissions in urban areas accumulate near the surface throughout the night (Doran et al., 2003; Garland and Branson, 1976; Pisano et al.,

Correspondence to: J. Stutz  
(jochen@atmos.ucla.edu)

1997). However, even in the stable NBL, trace gases are slowly transported vertically. During this slow transport, reactive compounds such as O<sub>3</sub> and NO undergo chemical transformations. Because the timescales of turbulent transport and chemical reactions are similar, nocturnal chemistry and vertical transport are closely linked, leading to complex vertical distributions of various trace gases and making nocturnal chemistry altitude dependent. The study of chemistry in the NBL, especially in polluted urban areas, is thus quite challenging (Geyer and Stutz, 2004a; Stutz et al., 2004b). The altitude dependence of both chemistry and vertical trace gas profiles vanish during the morning hours when surface heating leads to convection and accelerates vertical exchange (Doran et al., 2003; Garland and Branson, 1976; Pisano et al., 1997).

Few studies have thus far focused on the vertical variation of NBL chemistry. Night-time vertical distributions of O<sub>3</sub> have been measured in various rural and urban environments by tethered balloons, masts, and aircraft over a wide range of altitudes in the lower troposphere (Aneja et al., 2000; Chen et al., 2002; Colbeck and Harrison, 1985; Doran et al., 2003; Galbally, 1968; Glaser et al., 2003; Gusten et al., 1998; Harrison et al., 1978; Neu et al., 1994; Van Dop et al., 1977; Zhang and Rao, 1999). The results generally show positive vertical O<sub>3</sub> gradients, with higher O<sub>3</sub> concentrations at higher altitudes (Aneja et al., 2000; Galbally, 1968; Gusten et al., 1998; Van Dop et al., 1977; Zhang and Rao, 1999). Due to dry deposition (Colbeck and Harrison, 1985; Gusten et al., 1998; Harrison et al., 1978), reaction with surface emitted NO (Gusten et al., 1998), and inefficient vertical transport, O<sub>3</sub> is often depleted at the bottom of the NBL. O<sub>3</sub> above the nocturnal inversion is cut off from major sinks and is preserved at night. When the inversion begins to break up in the morning, rapid downward transport from the RL helps to restore the surface O<sub>3</sub> (Gusten et al., 1998; Kleinman et al., 1994; McKendry et al., 1997; Neu et al., 1994; Zhang and Rao, 1999). This has been confirmed by observations of a strong correlation between night-time O<sub>3</sub> in the RL and the maximum surface O<sub>3</sub> on the next day (Aneja et al., 2000; Zhang and Rao, 1999). Significant downward mixing of O<sub>3</sub> from the RL can contribute about half of the observed morning increase in surface O<sub>3</sub> concentrations in some cases (Kleinman et al., 1994; McKendry et al., 1997; Neu et al., 1994). In areas with good daytime ventilation to prohibit multi-day buildups of locally produced O<sub>3</sub>, the impact of this downward mixing is significant even during the late day hours. The study of Fast et al. (2000) shows that the entrainment from the RL reservoir into the growing convective boundary layer could contribute 20 to 40% of the afternoon surface O<sub>3</sub> levels in Phoenix valley.

Recently, simultaneous measurements of multiple chemical species and meteorological parameters have been carried out to provide more information about the NBL. Vertical distribution measurements of O<sub>3</sub>, NO<sub>2</sub>, temperature and relative humidity in a suburban area show persistent vertical profiles

for several hours after sunrise in some cases (Pisano et al., 1997). A similar trend has been found in the vertical profiles of O<sub>3</sub>, NO<sub>2</sub>, NO<sub>x</sub>, selected VOCs and meteorological parameters after very stable nights at a rural site (Glaser et al., 2003). A field study near Houston, TX, revealed frequent negative NO<sub>2</sub> and positive O<sub>3</sub> vertical gradients when temperature inversions and calm wind conditions were encountered (Stutz et al., 2004b). In addition, NO<sub>3</sub> showed positive vertical gradients in the stable NBL (Stutz et al., 2004b), which agrees with earlier NO<sub>3</sub> measurements in the lower boundary layer (Aliwell and Jones, 1998; Friedeburg et al., 2002). Modeling studies attribute positive vertical gradients of both O<sub>3</sub> and NO<sub>3</sub> mainly to the reactions with surface-emitted NO and VOCs (Fish et al., 1999; Geyer and Stutz, 2004a; Stutz et al., 2004b). Vertical profiles of N<sub>2</sub>O<sub>5</sub>, which depend on temperature profiles as well as NO<sub>2</sub> and NO<sub>3</sub> distributions, also develop in the stable NBL (Geyer and Stutz, 2004a; Stutz et al., 2004b). As a consequence of the vertical profiles of O<sub>3</sub>, NO<sub>3</sub> and N<sub>2</sub>O<sub>5</sub>, the loss of VOCs through direct oxidation and loss of NO<sub>x</sub> through surface uptake of N<sub>2</sub>O<sub>5</sub> become altitude dependent as well. A 1-D chemical transport model study reproduced the general features of these vertical profiles observed in field campaigns. The study also pointed out that N<sub>2</sub>O<sub>5</sub> vertical transport plays an important role for the radical chemistry at night (Geyer and Stutz, 2004a; Stutz et al., 2004b).

These studies clearly show that chemistry in the stable NBL is height dependent. Vertical profiles of trace gases and their chemistry are complex and dependent upon meteorological conditions. As a consequence, measurements of trace gases at single altitudes are not representative for the entire NBL. The lifetime and the budget of reactive species cannot be simply derived from single-altitude measurements alone. In addition, high levels of O<sub>3</sub> and NO<sub>3</sub> in the upper NBL lead to chemical processes that occur aloft well before they are present at the surface during morning hours. This effect is not well considered in current measurement strategies. Therefore, comprehensive observations of boundary layer vertical distributions of both reactive species and meteorological parameters during night-time and even morning hours are required for a better understanding of the height-dependent nocturnal chemistry system and the consequent influence on daytime chemistry.

However, very few studies on this topic have been made thus far, and most of them were carried out in suburban or rural areas. The height-dependent nocturnal chemistry in urban areas with strong surface emissions has been paid surprisingly little attention. Large uncertainties greatly limit our ability to qualitatively and quantitatively describe the complex interaction of chemistry with meteorology in a heavily polluted NBL. For example, the removal of O<sub>3</sub> as well as its precursors, VOCs and NO<sub>x</sub>, involves various height-dependent chemical processes, which are currently only known based on surface measurements. Night-time surface emissions in strongly polluted areas can result in surface

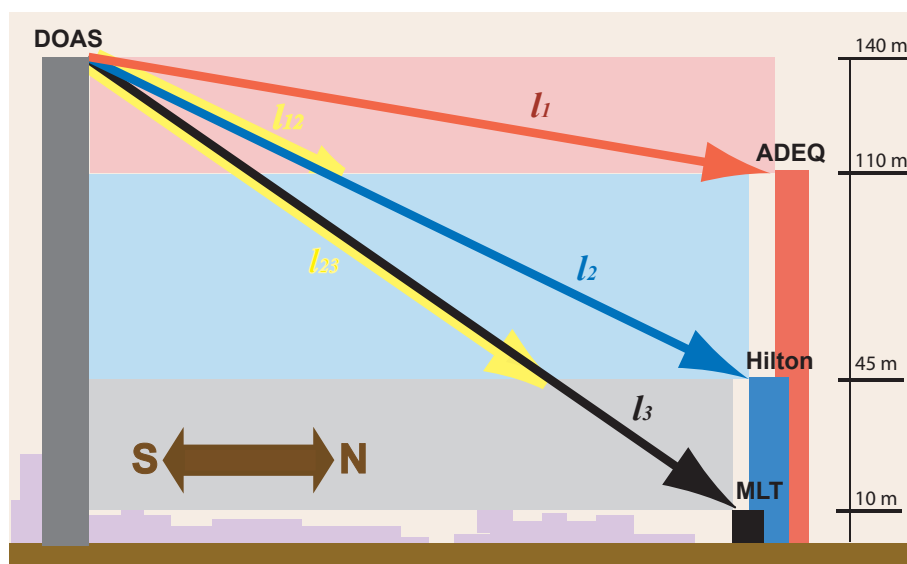


**Fig. 1.** Schematics of the DOAS light paths in Phoenix. The figure also shows the height intervals for which average concentrations were retrieved. The parameters in the figures are explained in detail in Sect. 2.2 and Table 1. The red rectangle refers to the upper box, blue refers to middle box and gray refers to lower box.

accumulation of O<sub>3</sub> precursors. The budgets of both O<sub>3</sub> and its precursors in the NBL and the ultimate influence of the height-dependent system of emissions, chemistry, and vertical transport in the NBL on daytime O<sub>3</sub> levels are not clear. As predicted by a recent chemical transport model study by our group (Geyer et al., 2003; Geyer and Stutz, 2004a), high surface NO emissions in urban areas are expected to influence both the vertical profiles and budgets of the core species of nocturnal chemistry such as O<sub>3</sub>, NO<sub>2</sub>, NO<sub>3</sub> and N<sub>2</sub>O<sub>5</sub>. In order to provide field data to test the predictions as well as to study the budget of various nocturnal trace gases in polluted urban areas, vertical distributions of a series of trace species as well as meteorological parameters were measured simultaneously during a field campaign in downtown Phoenix in summer 2001. Here we present these observations and discuss the vertical variations of the related chemical processes and the implications for O<sub>3</sub>–NO<sub>x</sub> system in the stable NBL.

## 2 Experimental section

In June 2001, a field experiment funded by the U.S. Department of Energy was conducted in the downtown area of Phoenix, AZ. Measurements were made at various locations in the city including the roofs of several high-rise buildings. UCLA's long-path Differential Optical Absorption Spectroscopy (DOAS) system was operated to provide 24-h continuous measurements of vertical distributions of a number of trace species in the open atmosphere. Meteorological parameters such as relative humidity (*RH*), wind direction and speed were monitored at various fixed altitudes. Potential temperature profiles were measured using balloon

sondes. In addition, in situ measurements of NO were made at different altitudes. This section provides details of the instrumental setup and the data analysis.

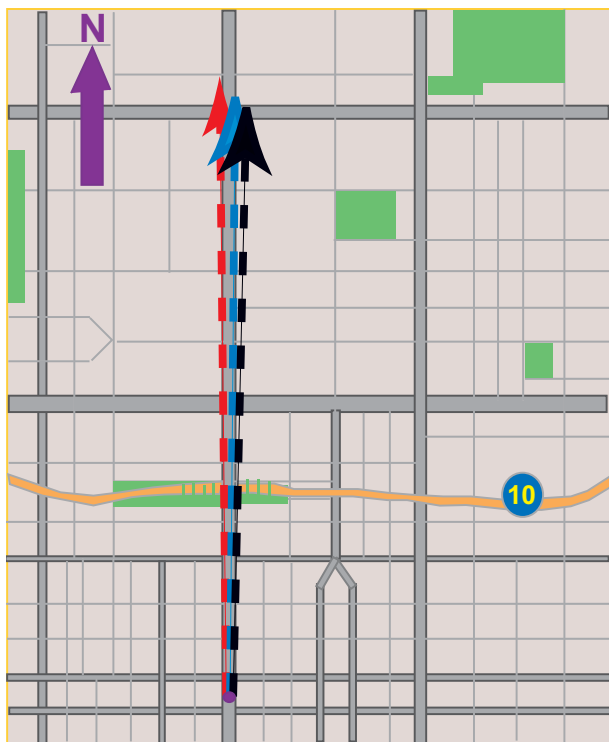
### 2.1 DOAS measurements

DOAS is a technique that identifies and quantifies trace gases by their distinctive UV-visible narrow band absorption structures in the open atmosphere (Platt, 1994). The main advantage of DOAS is the absolute quantification of species at low concentrations without disturbing the composition of the observed air mass. The quantification is solely based on the measured optical density and the known absorption cross sections of the detected species. In addition, the absence of sampling problems and the insensitivity of its accuracy to the presence of aerosols make this technique ideal for observations in the polluted atmosphere.

During this two-week field experiment (16 June 2001–1 July 2001), the UCLA long path DOAS instrument was set up on the 39th floor of BankOne, the highest building in downtown Phoenix, about 140 m above the ground level (Figs. 1 and 2). Details of the instrument can be found in Alicke et al. (2002). In short, light from a 500 W Xe-arc lamp was fed into a 1.5 m double Newtonian telescope, which was used to send a highly collimated light beam into the open atmosphere and to collect the light reflected back by arrays of quartz cube-corner prisms (retroreflectors). Three retroreflector arrays were mounted on the roofs of separate buildings (ADEQ, Hilton, and MLT) at a distance about 3.3 km north of BankOne (see Fig. 1). The altitudes and lengths of these three light paths are listed in Table 1. The average trace

**Table 1.** Light paths and building heights at Phoenix site.

Instrument Setup Height (m)		Light Path		
DOAS telescope on BankOne	~140		Height (m)	Length (km)
Upper Retro on ADEQ	~110	Upper	110~140	$l_1=3.51 \times 2$
Middle Retro on Hilton	~45	Middle	45~140	$l_2=3.29 \times 2$
Lower Retro on MLT	~10	Lower	10~140	$l_3=3.23 \times 2$

**Fig. 2.** Map illustration of the DOAS light paths in downtown Phoenix. The lengths of the light paths are given in Table 1. The color coding of the paths is according to Fig. 1.

gas concentrations along each light path were monitored by sequentially aiming the telescope at the three retroreflector arrays. The duration of a typical measurement cycle covering all three light paths was about 15–20 min depending on the atmospheric visibility.

Figures 1 and 2 illustrate that the light paths were superimposed in the horizontal but separated in the vertical direction. The paths ran along one direction of the street grid which connects the downtown and northern uptown regions of Phoenix. Because traffic was, to a large extent, spatially homogeneous in downtown Phoenix, the chance of inhomogeneities of trace gas distributions in the horizontal direction was expected to be small, particularly considering that the DOAS measurement averaged over 3.3 km. The in situ data of wind profiles at different altitudes provide additional help-

ful information for the possible influence of horizontal inhomogeneity (see Sect. 2.3). The buildings and structures along the light paths were mostly low (1–3 stories) except for the areas at the two ends of the paths. The area between downtown and uptown Phoenix therefore offers an ideal location for our measurements, since the impact of street canyons was expected to be small.

## 2.2 Data analysis

NO<sub>2</sub>, HONO, HCHO and O<sub>3</sub> were measured in the near UV spectral region according to their distinctive absorption structure in the wavelength range of 300–380 nm. NO<sub>3</sub> was detected separately at higher wavelengths (610–680 nm). The detailed spectra analysis procedures for the two spectral regions are described in Aliche et al. (2002), Geyer et al. (1999). Table 2 lists the spectral windows used for the analysis and the references for the literature absorption cross sections used in the analysis.

In order to study the vertical distribution of pollutants, the concentration results along light paths derived by the DOAS analysis need to be converted into concentrations averaged over distinct height intervals. The first step in this deconvolution process is to solve the temporal problem introduced by the sequential measurement. To account for the temporal variation during a measurement sequence, a linear function was used to interpolate the upper and middle light path data to the time of the lower light path measurements. The concentration at time  $t$  was derived with the concentrations at  $t_1$  (before  $t$ ) and  $t_2$  (after  $t$ ):

$$C_t = C_{t_1} + \frac{C_{t_2} - C_{t_1}}{t_2 - t_1} \cdot (t - t_1)$$

Here we assumed that during the short time period between scans (at most ~35 min), the change of trace gas concentrations can be approximated by a linear function. The results from measurement cycles longer than 35 min were filtered out in the calculation. While this is generally a good approximation for long-path data, during periods with rapid concentration changes this approach may lead to inaccurate results. However, these time periods can be easily identified based on the original data and excluded.

The trace gas concentrations averaged over three height intervals ( $C_{up}$ ,  $C_{mid}$ , and  $C_{low}$ ) were then derived using the

**Table 2.** Detection limits for each measured trace gas.

Species	Fitting window (nm)	Literature of absorption cross sections	Average Detection Limit (2σ)		
			Upper box (110–140 m)	Middle box (45–110 m)	Lower box (10–45 m)
NO <sub>2</sub>	336~371	Voigt et al. (2002)	0.11 ppb	0.18 ppb	0.64 ppb
HONO	336~371	Stutz et al. (2000)	0.04 ppb	0.07 ppb	0.25 ppb
HCHO	303~326	Meller and Moortgart (2000)	0.23 ppb	0.38 ppb	1.4 ppb
O <sub>3</sub>	303~326	Bass and Paur (1984)	1.7 ppb	2.8 ppb	10 ppb
NO <sub>3</sub>	617~668	Sander (1986)	3.5 ppt	6.0 ppt	18 ppt

following equations based on concentrations averaged along each light path ( $C_1$ ,  $C_2$ , and  $C_3$ ).

$$C_{\text{up}} = C_1$$

$$C_{\text{mid}} = \frac{C_2 \cdot l_2 - C_1 \cdot l_{12}}{l_2 - l_{12}}$$

$$C_{\text{low}} = \frac{C_3 \cdot l_3 - C_2 \cdot l_{23}}{l_3 - l_{23}}$$

The length variables  $l_2$ ,  $l_3$ ,  $l_{12}$ , and  $l_{23}$  are defined in Fig. 1.  $C_{\text{up}}$ ,  $C_{\text{mid}}$ , and  $C_{\text{low}}$  are not only averaged in the vertical, but also in the horizontal direction. Figure 1 illustrates the three boxes of air mass over which the averaging occurs. For the remainder of this paper, we assume that the differences in  $C_{\text{up}}$ ,  $C_{\text{mid}}$ , and  $C_{\text{low}}$  are dominated by the vertical variations in the concentrations. The validity of using multi-angle long path DOAS measurements to estimate vertical profiles was discussed in detail in (Stutz et al., 2002, 2004b) and is not repeated here.

Due to the error propagation through the calculation and the difference in light path lengths,  $C_{\text{low}}$  generally has larger errors and higher detection limits than  $C_{\text{up}}$  and  $C_{\text{mid}}$ . The mean detection limits in all height intervals for each measured species are listed in Table 2. All errors are reported as one standard deviation  $\sigma$  (Stutz and Platt, 1996). The reported detection limits are twice the errors.

Based on these results, the overall vertical gradients of trace gas concentrations between 27.5 m and 125 m altitude can be estimated with a linear approximation,

$$\frac{\Delta C}{\Delta z} = \frac{C_{\text{up}} - C_{\text{low}}}{z_{\text{up}} - z_{\text{low}}}$$

where  $z_{\text{up}}$  and  $z_{\text{low}}$  refer to the central height of the upper and lower box respectively (i.e., 125 m and 27.5 m). Our earlier studies show that the vertical trace gas profiles in the NBL show complex non-linear shapes. The gradient calculated in this equation is thus only used as a qualitative approach to illustrate the general features of our measured time series, rather than a quantitative description of the profiles.

Since the trace gas concentrations resulted from spectra fitting and the above-mentioned derivation procedure, negative values may appear when the actual concentrations were below DOAS detection limits, especially for the lowest height interval. To estimate the vertical gradient with real physical meaning, the negative concentration values were set to zero when calculating ( $C_{\text{up}} - C_{\text{low}}$ ).

### 2.3 In situ measurements

Meteorological parameters such as *RH*, temperature, wind speed and direction were continuously monitored close to the retroreflectors on top of the buildings with Campbell Scientific Inc. weather stations. Since the observation of vertical profiles with the long path DOAS technique is based on the assumption that there is no influence from horizontal advection at different altitudes, the wind profiles measured at different altitudes provide a useful reference to exclude cases when inhomogeneities in the horizontal advection contribute to the gradients (Fast et al., 2005). Potential temperature profiles which indicate the NBL stability and height were also provided by balloon soundings during selected nights. The balloons were launched from the Vehicle Emission Laboratory, 7 km east of BankOne (Doran et al., 2003). On the 39th and 16th floor of the BankOne building, NO and CO mixing ratios were measured by chemiluminescence (Thermo Environmental 42S) and gas filter correlation IR, which helps evaluate the relative emission strength at the surface (Doran et al., 2003). A ground-based air quality monitoring station of Arizona Department of Environmental Quality monitored continuously the main meteorological parameters and mixing ratios of air pollutants such as CO, NO<sub>x</sub> and O<sub>3</sub> at ground level in central Phoenix, approximately 3 km from BankOne, in a southwesterly direction. The photolysis rate of NO<sub>2</sub> ( $J_{\text{NO}_2}$ ), an indicator of the solar radiation strength, was monitored by a filterradiometer (Meteoconsult) at the Vehicle Emission Laboratory.

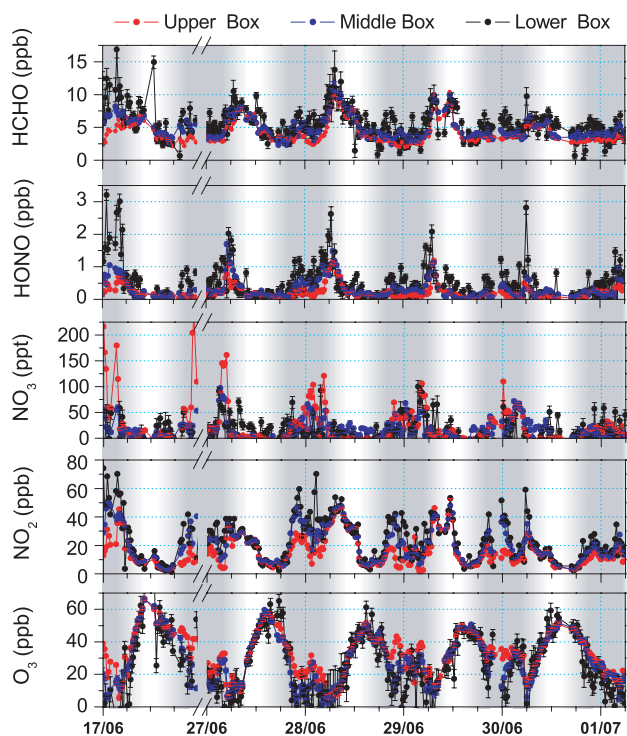


**Fig. 3.** Overview of the vertical profiles of measured trace species during 17 June–1 July 2001 in Phoenix. The background is shaded to draw attention to the nocturnal data. Gray and white denote nighttime and daytime, respectively. The transition between the colors shows sunrise and sunset periods. Lines in different colors show the time series of average trace gas mixing ratios at different height intervals (see Fig. 1 and Table 2 for details of the height intervals). We will use the same color coding for all the following figures. The length of the error bars is one standard deviation.

### 3 Measurement results

#### 3.1 Overview of vertical variations of measured species

An overview of the measured vertical profiles of trace gases is shown in Fig. 3. In general, clear vertical variations of trace gas levels in the three height intervals were observed during most nights in this experiment. O<sub>3</sub> mixing ratios in downtown Phoenix showed diurnal variations typical for polluted urban areas, with daytime maxima of up to 70 ppb and completely depleted O<sub>3</sub> on some nights. This variation is reversed in the NO<sub>2</sub> time series, which showed low NO<sub>2</sub> levels below 10 ppb during the day and maxima of up to 70 ppb at night. During all the nights shown in Fig. 3, strong vertical variations of NO<sub>2</sub> and O<sub>3</sub> mixing ratios were observed. The negative NO<sub>2</sub> gradient and positive O<sub>3</sub> gradient agree well with earlier observations in various rural and suburban areas (Glaser et al., 2003; Pisano et al., 1997; Stutz et al., 2004b), but with significantly larger magnitudes due to the higher emission rates in downtown Phoenix. The gradients

were sustained until the morning hours and then gradually disappeared after the onset of convective mixing.

NO<sub>3</sub>, which is formed by the reaction of NO<sub>2</sub> with O<sub>3</sub> and removed mainly by its reaction with ground-level emitted NO<sub>x</sub> and VOCs, also developed strong positive vertical gradients during most nights. The magnitude of both NO<sub>3</sub> mixing ratios and vertical gradients depends on the levels of NO<sub>2</sub> and O<sub>3</sub>. During the night of 30 June–1 July, for example, NO<sub>2</sub> levels were relatively low, indicating a weaker NO<sub>x</sub> emission strength compared with other nights. Accordingly, NO<sub>3</sub> levels were only slightly above the detection limits due to the low production rate and showed little gradient as a result of the low NO emission from the surface. This behavior is in agreement with the results of (Geyer and Stutz, 2004a; Hov, 1983). It should be noted that surprisingly high NO<sub>3</sub> levels were observed in Phoenix, with nocturnal maxima between 50–200 ppt. While the cause of this high NO<sub>3</sub> will be discussed further below, it is worth pointing out that the unique meteorological conditions in Phoenix could play a role. Daytime temperatures reached above 40°C and cooled down to minima of 25–30°C at night. The RH was below 20% during the day and below 40% during the night, except for 26 June when RH reached 70%. Both high temperatures and low RH are favorable for the development of high NO<sub>3</sub> levels due to the decreased importance of N<sub>2</sub>O<sub>5</sub> and its surface uptake (Geyer and Stutz, 2004a; Hov, 1983).

HONO, which is directly emitted from traffic and chemically formed in the atmosphere mainly by the heterogeneous hydrolysis of NO<sub>2</sub> on various surfaces (Finlayson-Pitts et al., 2003; Stutz et al., 2004a), showed negative vertical gradients. Because the gradients are of the same sign as those of NO<sub>2</sub>, it is difficult to discriminate between the different sources of HONO. However, the negative gradients of HONO together with its gradual accumulation during night, with the highest HONO levels in the later part of the night, point to a formation close to the surface. In some cases, the HONO gradients persisted a few hours after sunrise when photolysis production of OH started. Since HONO is an important OH source in the morning, leading to a significant increase of O<sub>3</sub> concentrations in the polluted boundary layer (Alicke et al., 2002; Aumont et al., 2003), the vertical gradient of HONO and its implications will be investigated further in an upcoming publication.

Significant negative vertical gradients of HCHO up to 0.12 ppb/m were observed during the night in Phoenix (for example the early morning of 17 June in Fig. 3). Since the photochemical production pathways of HCHO are absent at night, this strong HCHO profile implies the existence of another significant source, which should be active close to the ground. In earlier traffic tunnel measurements, significant amounts of primary HCHO from auto exhaust were observed (Kurtenbach et al., 2002). The night-time traffic in downtown Phoenix could therefore be a major emission source for HCHO. Although we have little information on the emission ratio of HCHO/NO<sub>x</sub> in the vehicle exhaust and the other

possible sources responsible for the high night-time HCHO emission in Phoenix, it can be concluded based on the observations that photochemistry is not the only major source for atmospheric HCHO. Future studies, for example tunnel measurements of emission ratios of HCHO, are suggested to quantify the contribution of direct emissions to the nocturnal atmospheric HCHO in urban areas.

The observed general patterns of trace gas vertical profiles in the NBL agree well with earlier modeling studies for typical urban cases (Geyer and Stutz, 2004a). According to the model results, the shape of these vertical profiles depend predominantly on the nocturnal atmospheric stability and the surface emission rates of NO and VOCs. To validate these model predictions, we have selected two nights illustrating the impact of these factors on the NBL in Phoenix.

### 3.2 A case with strong surface emissions and high stability

The night of 16 June–17 June (Fig. 4) was one of the most polluted during the experiment. Levels of CO measured at ~50 m altitude at BankOne were above 1 ppm around midnight (not shown here). During most other nights, CO levels were high only during morning rush hour, which was absent on 17 June (Sunday). We attribute the unusually high CO levels on this weekend night to the heavy traffic caused by an event that occurred in the stadiums near downtown Phoenix. The strong emissions are also reflected by the in situ data of NO at BankOne, which will be further discussed in Sect. 4.1.

A strong temperature inversion and low wind speeds, indicated by the in situ meteorological data (Fig. 5), show that this night was also characterized by a high vertical stability of the NBL. The temperature difference between Hilton (~45 m) and ADEQ (~110 m) was about 3–5 K during most parts of the night, especially before 04:00. Wind speeds rarely reached above 2 m/s during this period. *RH* was as low as 5–20%. Potential temperature profiles by balloon soundings (Fig. 6) further demonstrate the surface inversion strength and the approximate height of the stable NBL. Both balloon soundings and in situ measurements show a decrease of the temperature inversion as the night proceeded, in particular after 04:00.

Due to the strong surface emissions and the high stability of the NBL, clear positive vertical gradients of O<sub>3</sub> and NO<sub>3</sub> and negative gradients of NO<sub>2</sub>, HONO and HCHO were observed throughout this night. The vertical profiles were particularly strong before 04:00. The high NO<sub>2</sub> levels of up to 80 ppb in the lower box during this period are in agreement with strong night-time NO<sub>x</sub> emissions and the conversion of NO into NO<sub>2</sub> through the reaction with O<sub>3</sub>. As a result, O<sub>3</sub> mixing ratios in the lower box ranged from below detection limits to at most 20 ppb, implying a surface O<sub>3</sub> depletion as reported in the earlier studies (Colbeck and Harrison, 1985; Cros et al., 1992; Gusten et al., 1998). Because the vertical mixing was greatly limited, smaller concentrations of NO<sub>2</sub> and larger concentrations of O<sub>3</sub> were expected

at higher altitudes, especially above the nocturnal inversion height. The potential temperature profile at midnight (Fig. 6) reveals that the strong surface inversion led to a stable NBL with a height of less than 100 m. The upper box, above the inversion height, was left in the RL and thus largely decoupled from the ground emissions. Consequently, trace gas mixing ratios in the upper box reflected the composition of the RL and were close to those during daytime. As shown in Fig. 4, the upper box O<sub>3</sub> levels were significantly higher than those of the lower and middle boxes with a maximum of over 50 ppb, resulting in a strong positive O<sub>3</sub> gradient of up to 0.4 ppb/m. NO<sub>2</sub> mixing ratios in the upper layer were in the range of 5–20 ppb, leading to negative NO<sub>2</sub> gradients as large as –0.6 ppb/m. The fact that the O<sub>3</sub> and NO<sub>2</sub> gradients have similar magnitudes but opposite signs will be discussed further below (see Sect. 4.2). For the other important night-time oxidant, NO<sub>3</sub>, surprisingly high levels over 200 ppt were observed in the upper box. The lower box NO<sub>3</sub> levels rarely reached above 50 ppt, leading to maximum NO<sub>3</sub> gradients of 2 ppt/m. As a consequence of the vertical profiles of both O<sub>3</sub> and NO<sub>3</sub>, a strong vertical variation of the atmospheric oxidation capacity within and above the NBL is expected. According to the studies of Geyer and Stutz (2004a, b), the stable NBL at midnight in an urban case with strong emissions can be subdivided into an unreactive ground layer, an unreactive upper layer above ~80 m and a reactive mixing layer centered around 50 m altitude. Our observations during this night agree well with those model study results.

From 04:00 to sunrise at about 05:30 (see photolysis rate ( $J_{\text{NO}_2}$ ) in Fig. 5), the vertical gradients were significantly reduced. The smaller temperature inversion and the higher wind speeds indicate a weaker stability. This early morning transition was described by Doran et al. (2003), who speculated that large scale convergence and resulting upward motions over the Phoenix valley was the cause for the increase in vertical mixing prior to sunrise.

After sunrise, radiative heating results in a quick breakup of the surface inversion. A well-mixed layer starts to grow upward from the surface. In this case, the convective layer grew up to ~100 m at 06:00. By 08:00, a typical convective boundary layer with a depth of a few hundred meters had developed. Consistent with this morning transition, the observed vertical variations in Fig. 4 started to regress after 05:00 and had disappeared completely by 08:00 due to the strong vertical mixing. In addition, as a result of the increasing photolysis, NO<sub>2</sub> and HONO levels decreased while O<sub>3</sub> was produced by photochemistry and its mixing ratios increased at all altitudes.

### 3.3 A case with weaker surface emissions and varying stability

The night of 26 June–27 June (Fig. 7), a typical weekday night, was characterized by relatively weaker surface emissions and different vertical stabilities than the previous case.

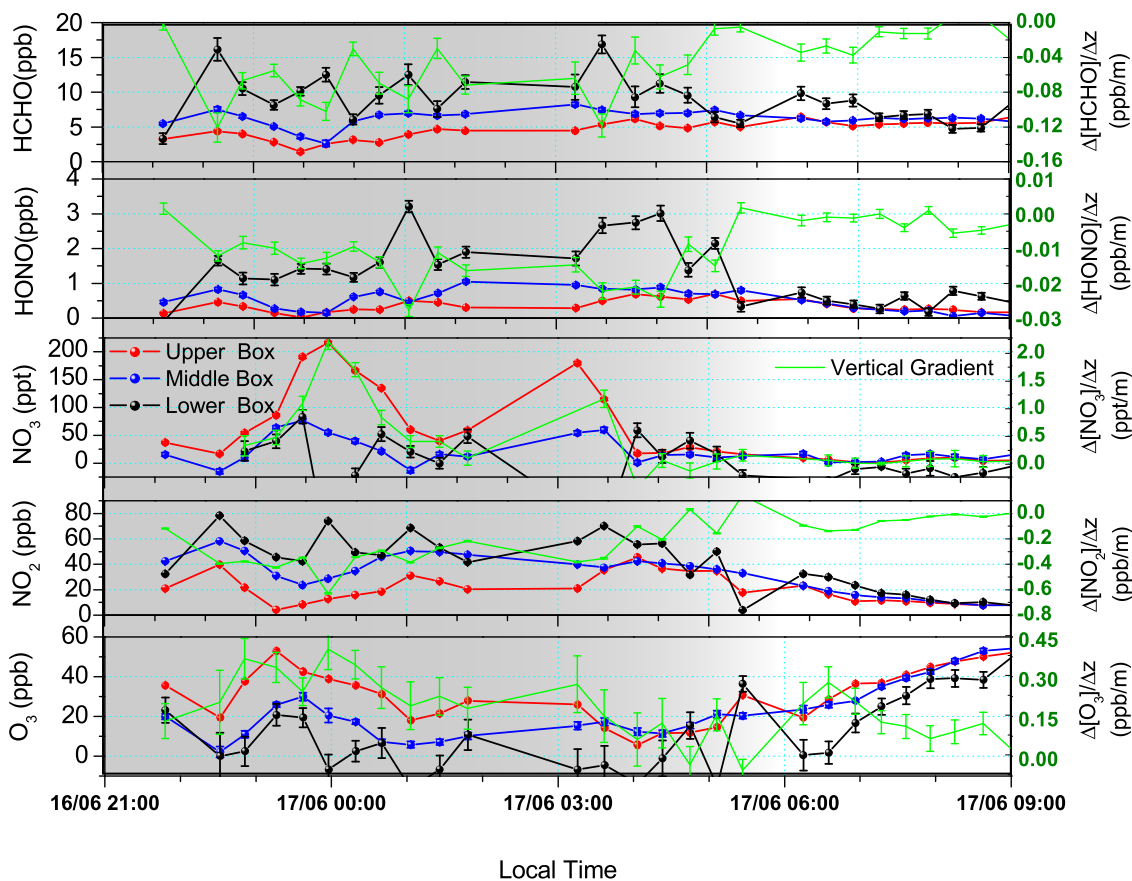


**Fig. 4.** Vertical profiles of trace gas distribution on the night of 16 June–17 June 2001. The left axis refers to the box-averaged mixing ratios. The right axis refers to the vertical gradients (green color) calculated based on the upper and lower box data.

CO mixing ratios were around 250 ppb until the onset of the morning rush hour, when they reached a maximum of near 800 ppb. Though the CO levels are also influenced by vertical transport, the predominant cause for the lower nocturnal CO levels than those of the night of 16 June–17 June, which included an evening event with high traffic levels, is the lighter traffic during typical weeknights in Phoenix. In addition, the measured temperature profiles and wind speeds on top of ADEQ generally show that this night showed weaker stability than 16 June–17 June (see Fig. 8). Accordingly, the observed trace gas vertical gradients on this night were clearly smaller than those of the high emission and high stability case.

The in situ meteorological data also illustrate two periods during this night with considerably different atmospheric stabilities (highlighted in Fig. 8): 1) A relatively unstable period with high wind speed around 4 m/s and no detectable temperature inversion from about 23:00 to 01:00. 2) A very stable period with very weak wind and a clear temperature inversion from 03:00 until 05:00. Because the difference in local emissions during the two periods is expected to have less impact (according to the in situ CO data), the difference

in vertical variations between these two selected periods was most likely caused by the different NBL stabilities. During the first highlighted period, the strong wind induced effective vertical mixing in the NBL, leading to negligible temperature gradients (Fig. 8). Consistent with the meteorological observations, the vertical trace gas gradients in Fig. 7 were undetectable or close to zero in these two hours. In addition, NO<sub>3</sub> levels were found to be close to zero during this time, most likely due to the efficient transport of surface emitted NO into higher altitudes where it destroyed NO<sub>3</sub>. This will be further discussed with calculated NO<sub>3</sub> production rate and steady state lifetime of NO<sub>3</sub> in Sect. 4.3. During the second period, wind speeds decreased to below 1 m/s and a clear temperature inversion developed (Fig. 8). Vertical mixing during this calm period was thus suppressed. Consequently the measured trace gas vertical gradients became stronger, reaching the maxima after 04:00 (Fig. 7). O<sub>3</sub> levels in the lower box rapidly decreased from ~20 ppb to zero through the reaction with surface emitted NO, while the levels in the middle and upper boxes remained approximately constant. Similarly, NO<sub>2</sub>, HCHO, and HONO mixing ratios in the lower box increased, while the levels in the other two boxes

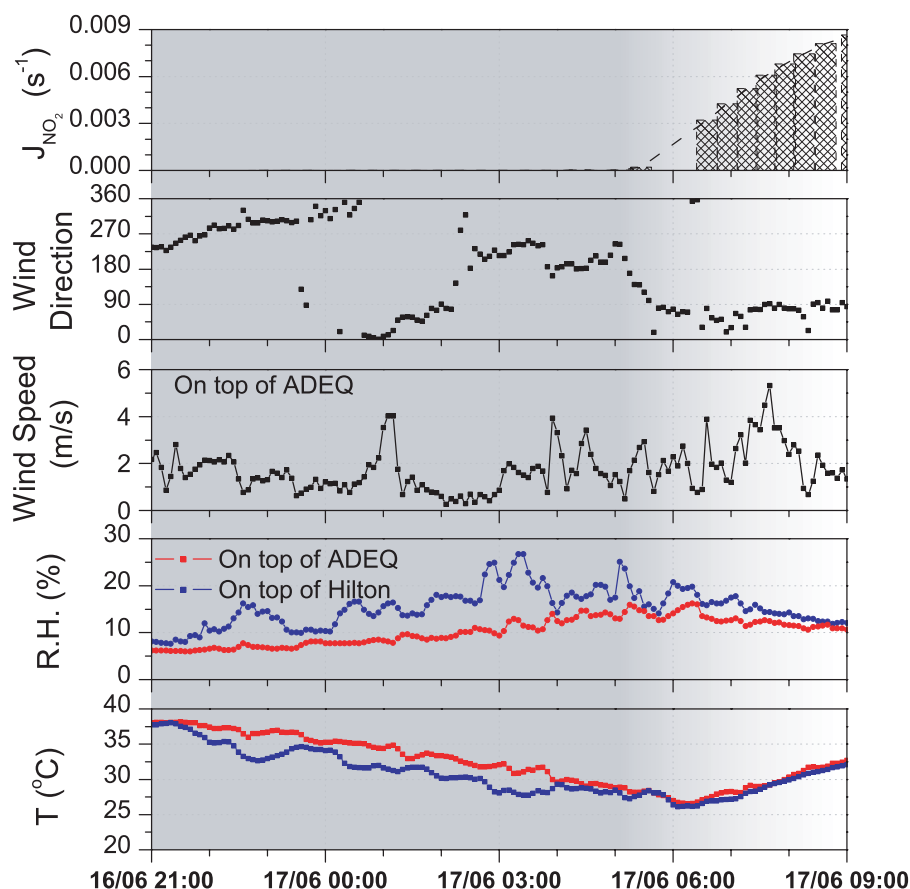


**Fig. 5.** Meteorological conditions on the night of 16 June–17 June 2001. ADEQ measurements were made at  $\sim 110$  m above the ground. Hilton data were taken at  $\sim 45$  m above the ground. For wind direction, north is 0 and east is 90 degree. The time series of the NO<sub>2</sub> photolysis frequency,  $J_{\text{NO}_2}$ , is included to show the time of sunrise.

had little change. With little NO being transported upward, the NO<sub>3</sub> level in the upper box increased rapidly and a maximum of  $\sim 150$  ppt was observed. After 05:00, an increase in wind speed again reduced the atmospheric stability and the vertical gradients of trace gases. Similar to the previous case, the vertical profiles disappeared completely after 08:00 when a typical convective boundary layer was established. The short term negative vertical gradients of NO<sub>2</sub>, HONO and HCHO about 1 h after sunrise reflect the weekday morning rush hour. Therefore, the behaviors of vertical gradients and the NBL stability during these two periods clearly show the influence of vertical mixing on the trace gas profiles.

#### 4 Discussion

Our observations of vertical trace gas profiles offer the unique opportunity to study the vertical variations of nocturnal chemistry as well as the budgets of O<sub>3</sub> and NO<sub>2</sub>. In this section, we will concentrate on the analysis of the budget of the O<sub>3</sub>-NO<sub>x</sub> system based on the observations. A detailed study of the chemical pathways in the NBL and the impact

**Table 3.** Key chemical reactions influencing the levels of O<sub>3</sub>, NO<sub>2</sub> and O<sub>x</sub> in the NBL.

(R1)	$\text{NO} + \text{O}_3 \rightarrow \text{NO}_2 + \text{O}_2$
(R2)	$\text{NO}_2 + \text{O}_3 \rightarrow \text{NO}_3 + \text{O}_2$
(R3)	$\text{NO}_3 + \text{NO} \rightarrow \text{NO}_2 + \text{NO}_2$
(R4)	$\text{NO}_3 + \text{VOCs} \rightarrow \dots \rightarrow \text{organic nitrate} + \text{other products}$
(R5)	$\text{NO}_3 + \text{NO}_2 + \text{M} \leftrightarrow \text{N}_2\text{O}_5 + \text{M}$
(R6)	$\text{N}_2\text{O}_5 + \text{H}_2\text{O} \xrightarrow{\text{aerosols}} 2\text{HNO}_3$

of vertical mixing by a chemical transport model will be presented in a forthcoming publication. The following section will give a brief review of the processes dominating the budgets of O<sub>3</sub>, NO<sub>2</sub>, and thus O<sub>x</sub> (the sum of O<sub>3</sub> and NO<sub>2</sub>) that will be used in the discussions. The involved key chemical reactions are summarized in Table 3.

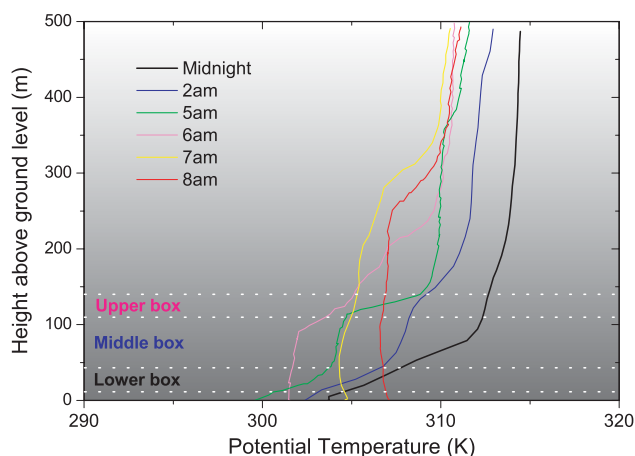


**Fig. 6.** Potential temperature profiles in the lower atmosphere on the night of 16 June–17 June 2001. The change of the strength and the depth of the potential temperature inversion with time illustrates the development of the stable NBL during the night and the growth of the convective boundary layer after sunrise.

#### 4.1 Nocturnal processes influencing O<sub>3</sub>, NO<sub>2</sub>, and O<sub>x</sub> levels

Due to the absence of sunlight, O<sub>3</sub> undergoes pure loss in the NBL. The dominant chemical sink of O<sub>3</sub> in urban areas with strong surface emissions is its rapid reaction with freshly emitted NO, a process known as NO titration (R1 in Table 3). However, this transformation of O<sub>3</sub> to NO<sub>2</sub> only temporarily removes O<sub>3</sub> from the boundary layer, since the photolysis of NO<sub>2</sub> during the next morning will lead to a re-release of O<sub>3</sub>. The photostationary state between NO, NO<sub>2</sub> and O<sub>3</sub> can be used to illustrate the impact of nocturnal NO emissions on the morning O<sub>3</sub> budget. The distribution between NO<sub>2</sub> and O<sub>3</sub> during the morning hours, ignoring photochemical chain production of O<sub>3</sub>, can be described by the Leighton ratio  $[O_3] = \frac{J_{NO_2}}{k_1} \cdot \frac{[NO_2]}{[NO]}$  (Finlayson-Pitts and Pitts, 2000), which includes a dependence on the photolysis rate of NO<sub>2</sub>. The sum of O<sub>3</sub> and NO<sub>2</sub>, O<sub>x</sub>, will remain constant, assuming the absence of O<sub>3</sub> or NO<sub>2</sub> loss processes other than (R1) and NO<sub>2</sub> photolysis. Based on the Leighton ratio, one can derive an expression for the steady state O<sub>3</sub> concentration before sunset and after sunrise, which depends on the levels of O<sub>x</sub>, NO<sub>x</sub> (NO+NO<sub>2</sub>), and J<sub>NO<sub>2</sub></sub>:

$$[O_3] = \frac{1}{2} \left( [O_x] - [NO_x] - \frac{J_{NO_2}}{k_1} + \sqrt{\left( [NO_x] - [O_x] + \frac{J_{NO_2}}{k_1} \right)^2 + 4 \frac{J_{NO_2}}{k_1} [O_x]} \right) \quad (1)$$

To determine the influence of nocturnal NO emissions, we start with the initial NO<sub>x</sub> concentrations at sunset, [NO<sub>x</sub>]<sub>ss</sub>. The sunrise NO<sub>x</sub> is thus defined by [NO<sub>x</sub>]<sub>sr</sub> = [NO<sub>x</sub>]<sub>ss</sub> + E<sub>NO</sub>, where E<sub>NO</sub> represents the total emissions of NO throughout

the night. The difference between O<sub>3</sub> levels at sunset and the next sunrise, [O<sub>3</sub>]<sub>sr</sub> – [O<sub>3</sub>]<sub>ss</sub>, shows the effective O<sub>3</sub> destruction due to nocturnal NO<sub>ss</sub> emissions assuming that J<sub>NO<sub>2</sub></sub> is equal in both cases. An O<sub>3</sub> destruction efficiency of NO emissions is defined as:

$$D_{O_3} = - \frac{\Delta[O_3]}{\Delta[NO_x]} = \frac{[O_3]_{ss} - [O_3]_{sr}}{E_{NO}}$$

The change in [O<sub>3</sub>] due to the increasing [NO<sub>x</sub>] (i.e., –D<sub>O<sub>3</sub></sub>) can be approximately expressed by the first order differentiation of Eq. (1):

$$\frac{\partial[O_3]}{\partial[NO_x]} = \frac{1}{2} \cdot \left( \frac{[NO_x] - [O_x] + \frac{J_{NO_2}}{k_1}}{\sqrt{([NO_x] - [O_x] + \frac{J_{NO_2}}{k_1})^2 + 4[O_x] \cdot \frac{J_{NO_2}}{k_1}}} - 1 \right) < 0 \quad (2)$$

Though the value of D<sub>O<sub>3</sub></sub> calculated with the above approximation depends on different combinations of [O<sub>x</sub>], [NO<sub>x</sub>], E<sub>NO</sub>, and J<sub>NO<sub>2</sub></sub>, it should be noted that the expression of Eq. (2) is always smaller than zero. The nocturnal emission of NO should thus always lead to lower O<sub>3</sub> levels at sunrise than those before the previous sunset in all cases (i.e., D<sub>O<sub>3</sub></sub> > 0).

The second order differentiation of Eq. (1),  $\frac{\partial^2[O_3]}{\partial[NO_x]^2} \approx \frac{\partial(-D_{O_3})}{\partial[NO_x]}$ , is positive. This further demonstrates that the O<sub>3</sub> destruction efficiency, D<sub>O<sub>3</sub></sub>, decreases with increasing NO<sub>x</sub> levels. Here we can discuss an example with [O<sub>x</sub>] = 60 ppb and J<sub>NO<sub>2</sub></sub> = 0.005 s<sup>–1</sup>. At low [NO<sub>x</sub>]<sub>ss</sub> levels (< 10 ppb) and low to moderate E<sub>NO</sub>, D<sub>O<sub>3</sub></sub> is found in the range of 0.7–0.9. At high levels of [NO<sub>x</sub>]<sub>ss</sub> (40 ppb), D<sub>O<sub>3</sub></sub> decreases to 0.4–0.5. Similarly, the magnitude of D<sub>O<sub>3</sub></sub> is also found to decrease with increasing E<sub>NO</sub>. Therefore, the impact of nocturnal NO emissions on the O<sub>3</sub> budget depends on various parameters and needs to be determined for every case separately. However, it is clear that (R1) does ultimately destroy O<sub>3</sub>, considering the difference in O<sub>3</sub> levels before sunset and after sunrise.

In addition to (R1), other processes influence the concentrations of O<sub>3</sub> and NO<sub>2</sub> in the NBL and change the total O<sub>x</sub> level directly. One may assume that the loss of one O<sub>x</sub> during night-time leads to exactly a loss of one O<sub>3</sub> in the next morning. However, Eq. (3) illustrates that, considering the effect of Leighton ratio Eq. (1), the reduction of O<sub>3</sub> is less than one.

$$\frac{\partial[O_3]}{\partial[O_x]} = \frac{1}{2} \cdot \left( \frac{[O_x] - [NO_x] + \frac{J_{NO_2}}{k_1}}{\sqrt{([NO_x] - [O_x] + \frac{J_{NO_2}}{k_1})^2 + 4[O_x] \cdot \frac{J_{NO_2}}{k_1}}} + 1 \right) < 1 \quad (3)$$

In the following, we will distinguish the above-discussed process, which converts O<sub>3</sub> into NO<sub>2</sub> without changing O<sub>x</sub> levels and influences the O<sub>3</sub> budget indirectly, from those that change the total O<sub>x</sub> and influence the O<sub>3</sub> budget directly.

The further oxidation of NO<sub>2</sub> forms NO<sub>3</sub> (R2) and temporarily destroys one O<sub>3</sub> and one NO<sub>2</sub>, i.e., two O<sub>x</sub> molecules. However, in urban areas the fast reaction of NO<sub>3</sub> with ground-level emitted NO is the major sink of NO<sub>3</sub>, and

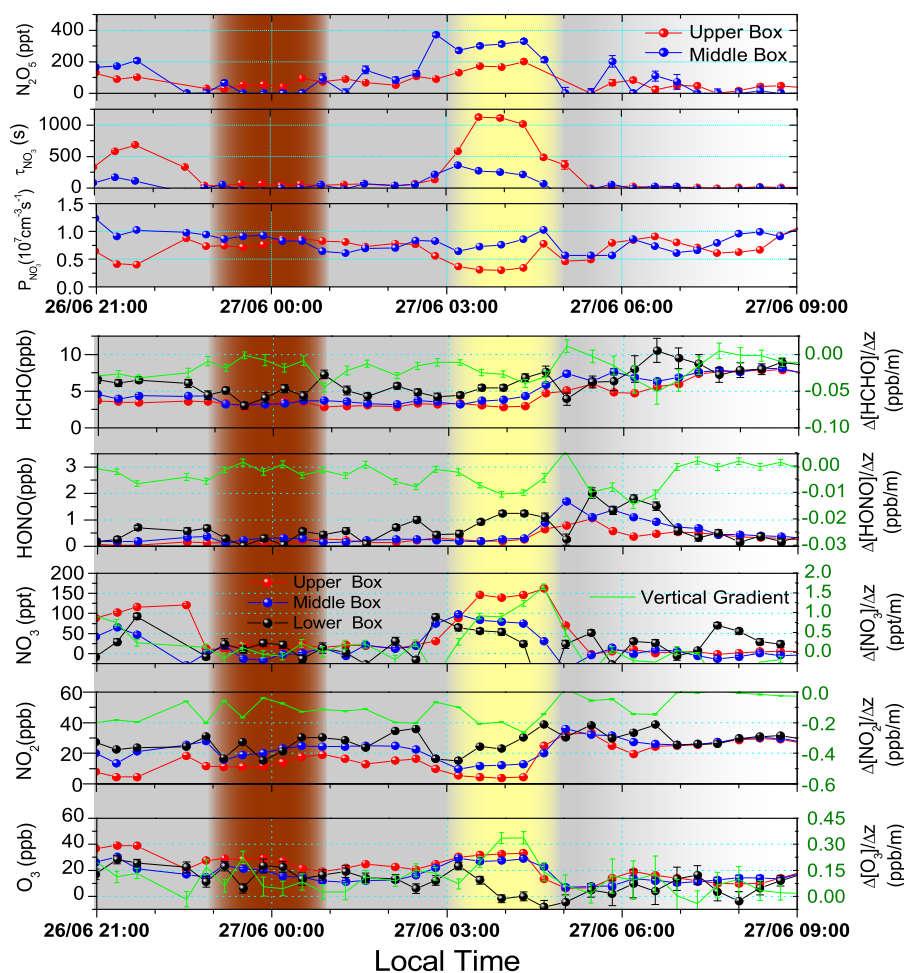


**Fig. 7.** Vertical profiles of trace gas distribution on the night of 26 June–27 June 2001. The lower panels illustrate the measured trace gas mixing ratios at three different height intervals and the calculated vertical gradients. The upper panels show the calculated NO<sub>3</sub> production rate  $P_{\text{NO}_3}$ , NO<sub>3</sub> chemical steady-state lifetime  $\tau_{\text{NO}_3}$ , and the steady-state N<sub>2</sub>O<sub>5</sub> levels in the upper and middle height intervals.

reforms two O<sub>x</sub> (R3). The total O<sub>x</sub> is thus conserved in the reaction system of (R2) and (R3) in the NBL, acting similarly to (R1) by converting O<sub>3</sub> into NO<sub>2</sub>. Therefore, only the transformations of NO<sub>3</sub> that do not regenerate O<sub>x</sub> can be considered a final loss of O<sub>x</sub>.

As one of the dominant oxidants in the NBL, NO<sub>3</sub> oxidizes various VOCs forming organic nitrates (R4). Although the further reactions of some organic nitrates can produce NO<sub>2</sub>, the majority of these reactions do not regenerate O<sub>x</sub> and thus lead to the ultimate O<sub>x</sub> loss (Stockwell et al., 1997). In addition, the reaction of NO<sub>3</sub> with NO<sub>2</sub> results in the formation of an important reservoir species, N<sub>2</sub>O<sub>5</sub>, through (R5). The uptake of N<sub>2</sub>O<sub>5</sub> on aerosols (R6) is an indirect sink for NO<sub>3</sub> and another loss process of O<sub>x</sub>. (R5) also consumes an additional O<sub>x</sub> in the form of NO<sub>2</sub>. It has to be noted that the efficiency of (R5) is strongly dependent on the ambient *RH*, which will be discussed further below.

The direct oxidation of VOCs by O<sub>3</sub> is slow compared to other O<sub>x</sub> loss processes and has little significance for the O<sub>x</sub> budget in urban areas.

Dry deposition of both NO<sub>2</sub> and O<sub>3</sub> on the ground and direct uptake on aerosols also lead to O<sub>x</sub> loss. The description of dry deposition in the urban NBL is challenging due to the poorly quantified vertical exchange rates and the simultaneously acting chemistry. Air quality models often employ a formalism describing deposition flux ( $j_{\text{dep}}$ ) by the product of a deposition velocity ( $v_{\text{dep}}$ ) at one altitude and the concentration of the trace gas ( $C$ ):  $j_{\text{dep}}=v_{\text{dep}}\times C$ . This formalism is often inaccurate for O<sub>3</sub> and NO<sub>2</sub> in urban areas due to the simultaneously acting chemical transformation of O<sub>3</sub> into NO<sub>2</sub> (R1) (Geyer and Stutz, 2004a; Hov, 1983).

Vertical transport of O<sub>3</sub> into and of NO<sub>2</sub> out of the NBL is a source and a sink of these gases in the NBL. We will discuss below how this process influences O<sub>x</sub> levels.

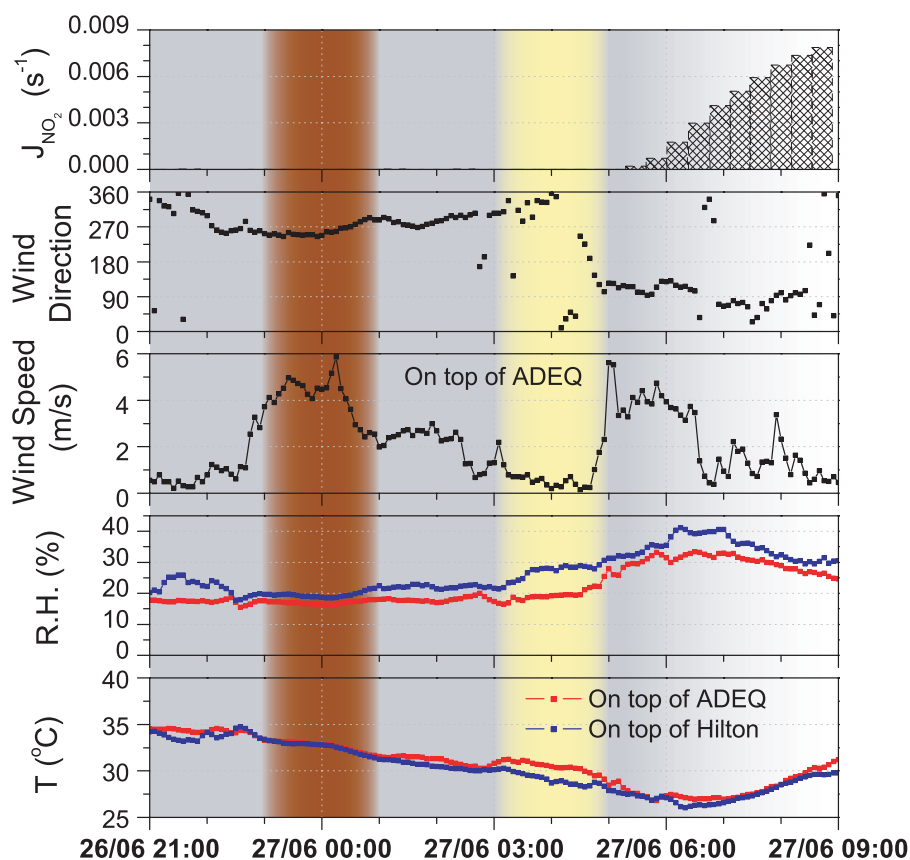


**Fig. 8.** Meteorological conditions on the night of 26 June–27 June 2001 (see caption of Fig. 5 for an explanation of the ADEQ and Hilton data). The brown bar indicates a period of low stability, while the yellow bar shows a period of strong stability.

Finally one also has to consider the direct emission of NO<sub>2</sub> through combustion processes. Since the emission ratio of NO<sub>2</sub>/NO<sub>x</sub> is typically less than 10%, the impact of direct emissions to the total O<sub>x</sub> budget in the NBL is, in most cases, small. However, it will be shown later that under some circumstances the influence of NO<sub>2</sub> emissions can be observed.

Based on the above discussions, it is clear that the analysis of the nocturnal O<sub>3</sub>, NO<sub>2</sub>, and O<sub>x</sub> budgets requires the separation of various processes that influence this system. In particular, processes that change O<sub>3</sub> and NO<sub>2</sub> levels without changing the level of O<sub>x</sub> need to be treated separately. Consequently, we will have a closer look at the NO titration process and the O<sub>3</sub>-NO<sub>2</sub>-O<sub>x</sub> system in Phoenix in Sect. 4.2. The contribution of NO<sub>3</sub> and N<sub>2</sub>O<sub>5</sub> chemistry, which plays an important role in the nocturnal O<sub>x</sub> loss and the ultimate O<sub>3</sub> removal, will be discussed in Sects. 4.3 and 4.4. Finally, a semi-quantitative calculation of the O<sub>3</sub>, NO<sub>2</sub> and O<sub>x</sub> budgets will be given in Sect. 4.5.

#### 4.2 The role of NO titration in the NBL chemistry

The first step to analyze the processes determining the NBL O<sub>3</sub> budget is the investigation of the role of reaction (R1).

The altitude dependence of nocturnal chemistry is controlled by the NO emission rate, in addition to the vertical stability of the NBL (Geyer and Stutz 2004a; and Hov, 1983). As shown in Sect. 3, night-time NO emissions followed by the fast NO titration led to positive O<sub>3</sub> vertical gradients and negative NO<sub>2</sub> gradients of similar magnitudes in Phoenix. It is thus interesting to discuss the vertical profiles of total O<sub>x</sub> in the NBL. Here, three different scenarios of observed nocturnal vertical profiles in Phoenix are discussed.

##### 4.2.1 The uniform O<sub>x</sub> vertical profile in a typical urban case in Phoenix

In a typical case in Phoenix, for example the night of 28 June–29 June 2001 (Fig. 9), clear vertical variations of O<sub>3</sub> and NO<sub>2</sub> levels were observed throughout the night until the onset of a strong morning vertical mixing, which agrees well with earlier observations (Aneja et al., 2000; Colbeck and Harrison, 1985; Glaser et al., 2003; Gusten et al., 1998; Zhang and Rao, 1999) and model simulations (Geyer and Stutz, 2004a; Hov, 1983). The O<sub>3</sub> and NO<sub>2</sub> gradients show a remarkable anti-correlation even during rapid variations (marked by the yellow arrows in Fig. 9). In contrast, the

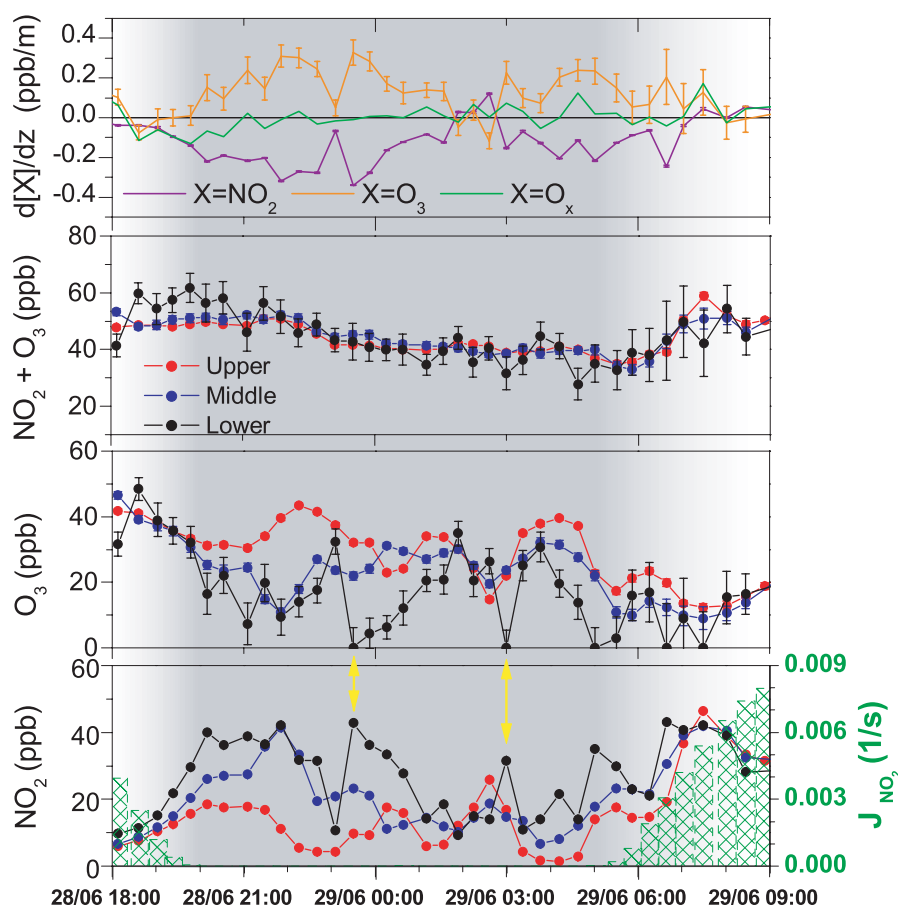


**Fig. 9.** Vertical profiles of NO<sub>2</sub> and O<sub>3</sub> on the night of 28 June–29 June 2001. The top panel shows the calculated vertical gradient of NO<sub>2</sub>, O<sub>3</sub>, and O<sub>x</sub>(O<sub>3</sub>+NO<sub>2</sub>) based on the upper and middle box data. The time series of J<sub>NO<sub>2</sub></sub>, photolysis frequency, indicates the time of sunset and sunrise.

calculated O<sub>x</sub> level does not show a detectable gradient during most parts of the night. The variations in NO<sub>2</sub> and O<sub>3</sub> in the time series are canceled out in the sum and are not reflected in O<sub>x</sub> levels. The only small variations of O<sub>x</sub> around 03:00–05:00 are believed to be introduced by horizontal advection, because the in situ meteorological data on top of the different buildings show consistent wind directions during this night except for some deviations at 03:00–05:00.

Following sunrise, O<sub>x</sub> levels increased, while O<sub>3</sub> concentrations remained low until 08:00 due to the large amount of freshly emitted NO during rush hour. This increase in O<sub>x</sub> but not in O<sub>3</sub> was most likely caused by the high direct emissions of NO<sub>2</sub> by traffic and the downward transport of O<sub>3</sub> from the RL followed by (R1). After 08:00, NO<sub>2</sub> mixing ratios decreased with reduced traffic and continuously increasing photolysis rate. Both O<sub>3</sub> and O<sub>x</sub> levels increased gradually as the photochemical O<sub>3</sub> formation process started to take over.

As stated earlier, surface NO emissions drive the height-dependent NO titration process. Because (R1) only converts

O<sub>3</sub> to NO<sub>2</sub> without changing O<sub>x</sub> levels, O<sub>x</sub> should have no vertical gradient if (R1) is the dominant chemical process in determining vertical distributions of both NO<sub>2</sub> and O<sub>3</sub>. Therefore, our observations in this scenario clearly demonstrate the dominant role of NO titration for the vertical variations of NBL chemistry during a typical polluted night in Phoenix. The similar anti-correlated profiles of NO<sub>2</sub> and O<sub>3</sub> were also observed in earlier studies at suburban areas with heavy traffic (Chen et al., 2002).

During the majority of the nights in this field campaign, negligible O<sub>x</sub> gradients similar to those in Fig. 9 were observed. However, there were exceptions during two nights: 16 June–17 June and 30 June–1 July, which need further discussions.

#### 4.2.2 Stronger surface emission case

During the night of 16 June–17 June (Fig. 10), which showed the strongest vertical gradients of trace gases during this two-week field study, the large vertical gradients of NO<sub>2</sub> and O<sub>3</sub>

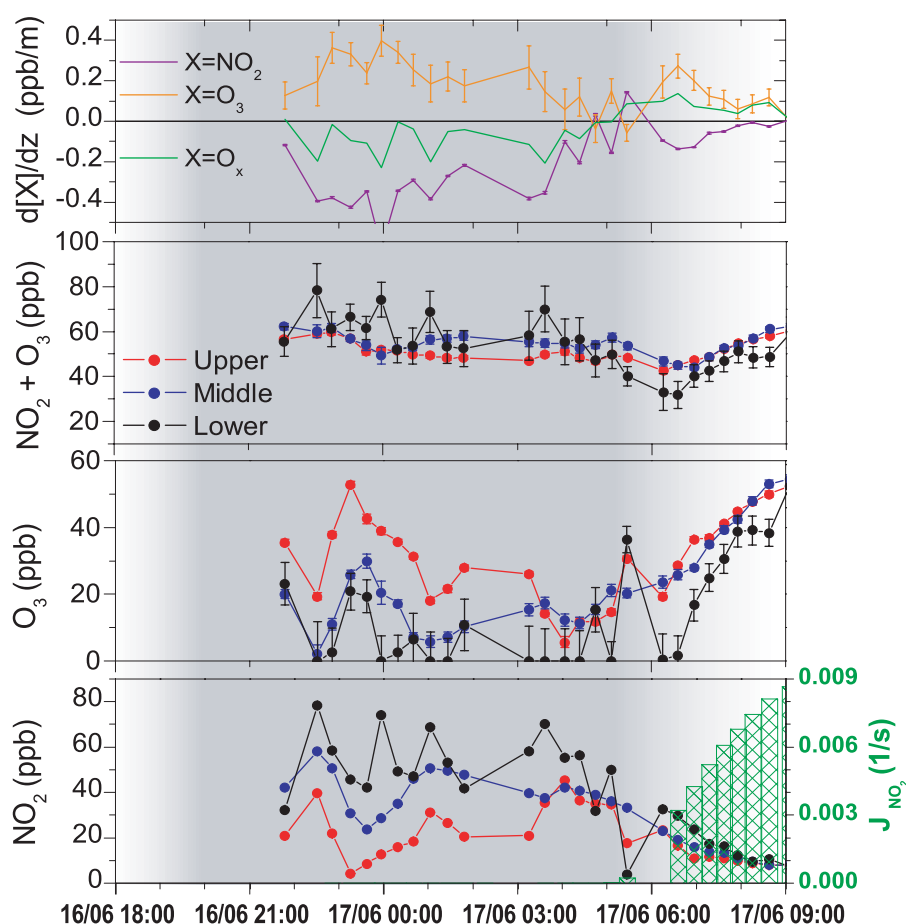


**Fig. 10.** Vertical profiles of NO<sub>2</sub> and O<sub>3</sub> on the night of 16 June–17 June 2001 (see caption of Fig. 9 for a more detailed explanation).

mostly canceled each other out as seen by the small O<sub>x</sub> gradient. The O<sub>x</sub> level in the lower box was, however, in general higher than that in the middle and upper boxes. As a result, the calculated O<sub>x</sub> vertical gradient was negative during most parts of the night. Considering the very high NO<sub>2</sub> levels and the surface O<sub>3</sub> depletion during this night, it is believed that particularly high ground-level emissions are responsible for this negative O<sub>x</sub> gradient.

Although NO emission rates were not directly monitored during this study, the mixing ratios of NO were measured at the ground level and on two floors of the BankOne building (Fig. 12). The night of 28 June–29 June, which showed the behavior of O<sub>x</sub> profiles similar to those during most other nights in Phoenix (Sect. 4.2.1), was a typical weekday night. The evening traffic in the city led to up to 30 ppb NO at the ground. Due to the extremely high daytime temperature in summer, the morning rush hour in Phoenix often occurs as early as around sunrise. The morning NO peak in Fig. 12 shows the early rush hour with a maximum at about 06:00. The delay in the NO maximum at higher altitudes was caused by the slow upward transport of NO. In contrast, the night of

16 June–17 June was a weekend night, from Saturday to Sunday. The morning rush hour NO peak is absent. However, high NO mixing ratios at both the ground level and 50 m altitude were observed during this night (Fig. 12), which was caused by increased traffic due to a sports event in downtown Phoenix.

As a result of the exceptionally high nocturnal NO emissions during 16 June–17 June and the rapid reaction (R1), large amounts of O<sub>3</sub> were converted into NO<sub>2</sub> in the lower NBL. The lower box NO<sub>2</sub> reached as high as 80 ppb during this night, which is about twice the maximum NO<sub>2</sub> level of the previous case. A large NO<sub>3</sub> production rate by (R2) is thus expected. In fact, this was the night with the highest NO<sub>3</sub> levels during this experiment. Above 200 ppt NO<sub>3</sub> were detected in the upper box, while the average maximum NO<sub>3</sub> level during the other nights was below 100 ppt. Because of the very active NO<sub>3</sub>-N<sub>2</sub>O<sub>5</sub> chemistry, NO<sub>2</sub> formation pathways other than NO titration (R1), such as (R3) and (R5), significantly influence the vertical distribution of O<sub>x</sub> in the NBL. In particular, the downward transport of N<sub>2</sub>O<sub>5</sub> and its thermal dissociation (R5) in the lower NBL can indirectly

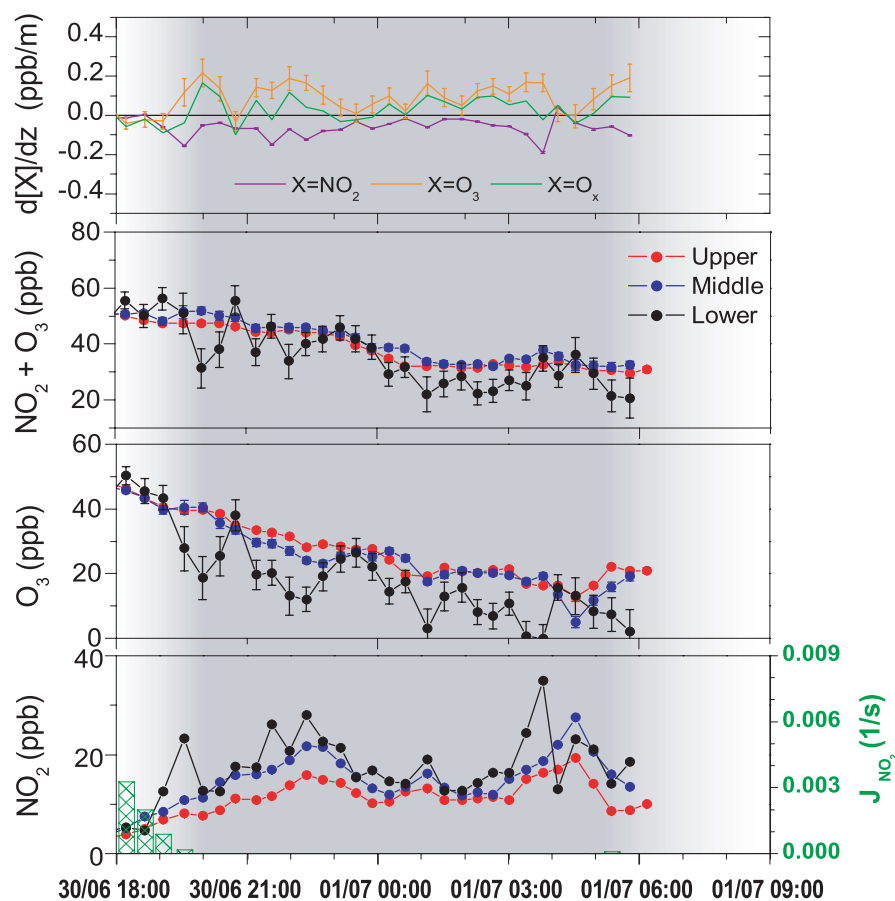


**Fig. 11.** Vertical profiles of NO<sub>2</sub> and O<sub>3</sub> on the night of 30 June–1 July 2001 (see caption of Fig. 9 for a more detailed explanation).

transport NO<sub>2</sub> and NO<sub>3</sub> from aloft to the surface (Geyer and Stutz, 2004a). Together with the rapid reaction of NO<sub>3</sub> with NO (R3), this mechanism leads to the formation of three NO<sub>2</sub> molecules for every N<sub>2</sub>O<sub>5</sub> molecule transported downwards. With the particularly high NO<sub>3</sub> mixing ratios observed during this night (Fig. 10), N<sub>2</sub>O<sub>5</sub> and its transport could contribute significantly to the high O<sub>x</sub> levels close to the ground. The direct emission of NO<sub>2</sub> at the surface is often unimportant due to the low NO<sub>2</sub>/NO<sub>x</sub> emission ratio (Kurtenbach et al., 2002). Although, the emissions were particularly strong in this case, a larger NO<sub>2</sub> deposition on the ground surface could counter balance or even outweigh the direct NO<sub>2</sub> emissions. Therefore, direct emissions most likely contributed little to the observed O<sub>x</sub> gradients. It should be noted that in this case dry deposition of O<sub>3</sub> is unimportant as a consequence of the high NO<sub>x</sub> emissions and fast O<sub>3</sub> depletion. Instead, dry deposition of NO<sub>2</sub> became significant as an indirect O<sub>3</sub> loss. Again, this loss could be counter balanced by strong direct NO<sub>2</sub> emissions. Whether the overall effect due to dry deposition, direct NO<sub>2</sub> emissions, and vertical transport lead to a net sink or source for O<sub>x</sub> in the NBL has to be discussed more quantitatively with the help of chemical transport models.

Nevertheless, the negative O<sub>x</sub> vertical gradient during the night of 16 June–17 June shows that in cases of very high surface NO<sub>x</sub> emissions, the dominance of the NO titration process is reduced and the idea of a constant vertical distribution of O<sub>x</sub> does not hold.

#### 4.2.3 Weaker surface emission case

In contrast, during the night of 30 June–1 July, another weekend night of Saturday to Sunday, the O<sub>x</sub> levels remained at slightly smaller values in the lower box than those of the two higher boxes (Fig. 11). A positive O<sub>x</sub> vertical gradient was present with values about half of the O<sub>3</sub> gradient.

Although horizontal advection cannot be completely excluded, a competitive O<sub>x</sub> sink must be present near the surface, leading to the positive O<sub>x</sub> gradient. Dry deposition of O<sub>3</sub>, which is unimportant when strong NO titration dominates in a polluted area, is a major cause of surface O<sub>3</sub> removal in rural areas (Geyer and Stutz, 2004a). Theoretically it could also contribute considerably in an urban case with light NO emissions. The comparison of in situ NO data (Fig. 12) shows much lower NO levels on 30 June–1 July than the previous two cases. The lower box NO<sub>2</sub>

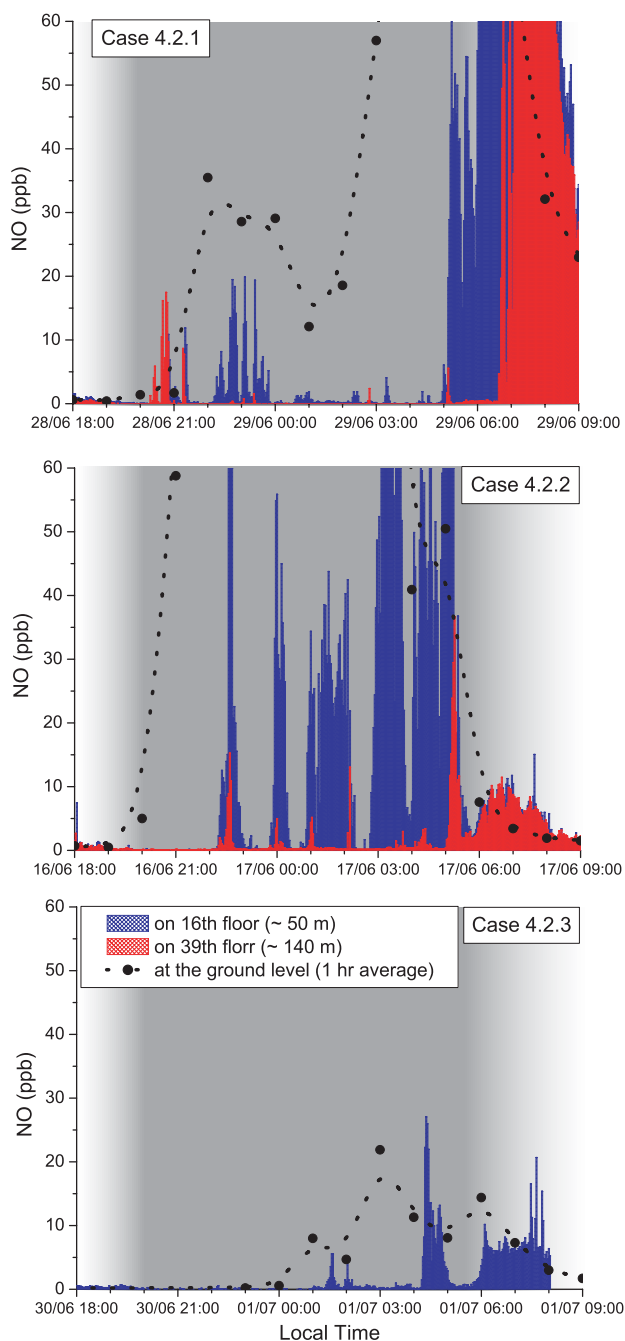


**Fig. 12.** Comparison of NO levels on nights of 16 June–17 June, 28 June–29 June and 30 June–1 July.

levels (Fig. 11) were only about half of those in the case of Sect. 4.2.1 (Fig. 9). In addition, the vertical gradients of both NO<sub>2</sub> and O<sub>3</sub> were also considerably smaller compared to the other cases. These observations all suggested weaker NO emissions during this night. The role of NO titration in the O<sub>x</sub> vertical distribution is thus weakened. With considerable levels of O<sub>3</sub> at the bottom of the NBL, dry deposition com-

peted with NO titration and resulted in an additional O<sub>3</sub> loss at the ground surface, which led to the lower total O<sub>x</sub> level in the lower box than aloft. While dry deposition can be important for the O<sub>x</sub> budget in urban areas, for example in this case, the fast NO titration causes the O<sub>3</sub> deposition velocity to change with height and thus makes the accurate estimation of this velocity for air pollution models challenging (Wesely and Hicks, 2000). It should be noted that NO<sub>2</sub> deposition and the resulting negative vertical flux to the ground surface was not considered in the above discussions.

#### 4.2.4 Comparison of the gradients in different cases

The comparison of these three cases clearly demonstrates the critical role of the surface emission strength in influencing the vertical structures of nocturnal chemistry in urban environments. The significance of NO titration and consequently the vertical distribution of O<sub>x</sub> vary with the surface emission strength.

It should be noted that besides the emission strength, the NBL stability also influences the vertical distribution of trace gases (see Sect. 3.3). Although the different surface emission strengths during these three nights ( $E_{16 \text{ June}–17 \text{ June}} > E_{28 \text{ June}–29 \text{ June}} > E_{30 \text{ June}–1 \text{ July}}$ ), contributed to some extent, in determining the difference in the magnitude of NO<sub>2</sub> and O<sub>3</sub> vertical gradients ( $\frac{dC}{dz}_{16 \text{ June}–17 \text{ June}} > \frac{dC}{dz}_{28 \text{ June}–29 \text{ June}} > \frac{dC}{dz}_{30 \text{ June}–1 \text{ July}}$ ), the factor of atmospheric stability must be considered as well. As shown in Fig. 5, the night of 16 June–17 June was characterized by very low wind speed mostly around 0–2 m/s and a strong temperature inversion of up to 5 K difference between the roof of ADEQ (110 m) and Hilton (45 m). Meteorological data from the other two nights show weaker atmospheric stability. The night of 28 June–29 June had a little higher wind speed and a relatively weaker temperature inversion. The temperature difference between the two buildings was at most 2 K. During the night of 30 June–1 July, no temperature inversion was observed and the wind speed was mostly above 3 m/s. Therefore, the NBL stability during these cases has the same order as that of the emission factor (Table 4). The difference in both emissions and atmospheric stability determined the different gradient magnitudes during these nights. A quantitative discrimination of these two factors, however, requires future model studies.

Despite the above-discussed differences, the three cases do have clear common features in the trend of O<sub>x</sub>. In all cases, O<sub>x</sub> mixing ratios gradually decreased with the development of the night and reached the lowest values around sunrise. A detailed discussion of the O<sub>x</sub> budget based on these data will be given in Sect. 4.5.

**Table 4.** Comparison of O<sub>x</sub> loss during nights with different stabilities and different emissions.

	Stability	Emission	d[NO <sub>2</sub> ]/dt ppb/h	d[O <sub>3</sub> ]/dt ppb/h	d[O <sub>x</sub> ]/dt ppb/h
16 June–17 June	Strong	Strong	–	–	–1.4±0.3
28 June–29 June	Medium	Medium	–	–	–1.9±0.1
30 June–1 July	Weak	Weak	–0.2±0.1	–2.3±0.1	–2.6±0.1

### 4.3 NO<sub>3</sub> chemistry in the urban NBL

The chemistry of NO<sub>3</sub> and its reservoir species N<sub>2</sub>O<sub>5</sub> has a strong influence on the fate of O<sub>x</sub>. Due to the vertical distributions of NO<sub>2</sub> and O<sub>3</sub> and the height-dependent reaction (R2), NO<sub>3</sub> also develops vertical gradients. The observations in Phoenix generally showed high NO<sub>3</sub> levels often above 50 ppt in the upper box, but small and often negligible levels close to the ground (see Fig. 3 in Sect. 3.1).

Figure 7 shows NO<sub>3</sub> vertical profiles for the night of 26 June–27 June, which was already discussed in Sect. 3.3 with respect to the influence of stability on vertical profiles. During periods of high stability in the early and late night, clear positive vertical gradients of NO<sub>3</sub> can be identified, which is consistent with the model prediction by Geyer and Stutz (2004a) for polluted urban cases. NO<sub>3</sub> mixing ratios reached up to 150 ppt in the upper box and decreased towards the ground. During the period with low NBL stability, however, NO<sub>3</sub> levels were low (0–30 ppt) at all altitudes. The vertical gradients were less distinct than those during the stable periods, mainly due to the increased vertical mixing. To understand the cause for this NO<sub>3</sub> behavior, the height dependence of NO<sub>3</sub> formation and loss are investigated in the following. To avoid the influence of the scatter of the lower box data as a result of temporal variations in the path-integrated data and the large errors of the lower box mixing ratios, we will focus on the data in the middle and upper boxes.

The opposite vertical distributions of NO<sub>2</sub> and O<sub>3</sub> lead to an altitude dependence of NO<sub>3</sub> formation through (R2). The NO<sub>3</sub> production rate,  $P_{\text{NO}_3} = k_2 \cdot [\text{NO}_2] \cdot [\text{O}_3]$  ( $k_2 = 1.4 \times 10^{-13} e^{-2470/T} \text{ cm}^3 \text{ s}^{-1}$ ; Atkinson et al., 2004), calculated based on measured mixing ratios of NO<sub>2</sub> and O<sub>3</sub>, showed values about  $0.5\text{--}1 \times 10^7 \text{ cm}^{-3} \text{ s}^{-1}$  during both stable and unstable periods (Fig. 7). The vertical gradient of P<sub>NO<sub>3</sub></sub> was weak and did not show a clear trend due to the opposite signs of O<sub>3</sub> and NO<sub>2</sub> gradients. However, a closer look at the dependence of P<sub>NO<sub>3</sub></sub> gradients on the NO<sub>2</sub> and O<sub>3</sub> distributions displays a systematic behavior of P<sub>NO<sub>3</sub></sub> profiles. Based on the important role of NO titration in typical urban areas (Sect. 4.2) and an assumption of linear vertical profiles of both NO<sub>2</sub> and O<sub>3</sub>, P<sub>NO<sub>3</sub></sub> at altitude *z* can be estimated with the concentrations at a reference altitude (i.e., [NO<sub>2</sub>]<sub>z<sub>0</sub></sub> and [O<sub>3</sub>]<sub>z<sub>0</sub></sub>) and the vertical gradients

( $\delta = d[\text{O}_3]/dz \approx -d[\text{NO}_2]/dz$ ) of NO<sub>3</sub> precursors:

$$P_{\text{NO}_3}(z) \approx k_2 \cdot ([\text{NO}_2]_{z_0} - \delta \cdot \Delta z) \cdot ([\text{O}_3]_{z_0} + \delta \cdot \Delta z) \quad (4)$$

The derivation of the vertical gradient of P<sub>NO<sub>3</sub></sub> reveals that the sign of the P<sub>NO<sub>3</sub></sub> gradient at a specific altitude is solely dependent on the comparison of NO<sub>2</sub> and O<sub>3</sub> concentrations. The product of the difference in [NO<sub>2</sub>]<sub>z</sub> and [O<sub>3</sub>]<sub>z</sub> levels and their vertical gradients  $\delta$  determines the magnitude of the P<sub>NO<sub>3</sub></sub> gradient:

$$\begin{aligned} \frac{dP_{\text{NO}_3}}{dz} &\approx k_2 \cdot \delta \cdot ([\text{NO}_2]_{z_0} - [\text{O}_3]_{z_0} - 2\delta \cdot \Delta z) \\ &\approx k_2 \cdot \delta \cdot ([\text{NO}_2]_z - [\text{O}_3]_z) \end{aligned} \quad (5)$$

Figure 7 shows generally lower NO<sub>2</sub> levels than those of O<sub>3</sub> in both upper and middle boxes. Consequently, P<sub>NO<sub>3</sub></sub> at these altitudes displayed a negative vertical gradient during most of the night. The largest gradient of P<sub>NO<sub>3</sub></sub> appeared when the NO<sub>2</sub> and O<sub>3</sub> profiles were strong (i.e., the high stability periods during 26 June–27 June) or when O<sub>3</sub> levels were considerably higher than those of NO<sub>2</sub> in the beginning of the night, which is also consistent with the expression of Eq. (5). In contrast, a very weak vertical gradient of P<sub>NO<sub>3</sub></sub> appeared during the period with low NBL stability as a result of a small  $\delta$  in Eq. (5).

Despite the presence of a negative vertical gradient of the NO<sub>3</sub> production rate, positive NO<sub>3</sub> gradients were observed. We thus discuss the NO<sub>3</sub> sink and the consequent steady state lifetime of NO<sub>3</sub>:

$$\tau_{\text{NO}_3} = \frac{[\text{NO}_3]}{\text{NO}_3 \text{ loss or production rate}} = \frac{[\text{NO}_3]}{k_2 \cdot [\text{NO}_2] \cdot [\text{O}_3]} \quad (6)$$

It has to be noted that this calculation is based on the steady state assumption of both NO<sub>3</sub> and its reservoir species N<sub>2</sub>O<sub>5</sub>, which is not always fulfilled in the atmosphere (Brown et al., 2003). Its accuracy depends on the ambient NO<sub>2</sub> level, the temperature, the levels of species reacting with NO<sub>3</sub> directly, and the vertical transport of the reservoir species N<sub>2</sub>O<sub>5</sub> which influences NO<sub>3</sub> distribution indirectly (Geyer and Stutz, 2004a). Here we use  $\tau_{\text{NO}_3}$  to gain insight into the general behavior of the altitude dependence of the loss processes of NO<sub>3</sub>. A more precise analysis requires the use of a chemical transport model.

$\tau_{\text{NO}_3}$  was considerably shorter in the lower NBL than aloft during times of high vertical stability on 26 June–27 June

(Fig. 7). It was in the range of 0–300 s for the middle box but reached 500–1200 s in the upper box. The much longer lifetimes in the upper box are clearly associated with the observed high NO<sub>3</sub> mixing ratios.

Due to the surface emissions and the negative vertical profile of NO (Sect. 4.2.1), the direct loss process of NO<sub>3</sub> through reaction (R3) is stronger near the ground. In particular, NO, the sink species of NO<sub>3</sub>, is converted into NO<sub>2</sub> as it is transported upward and has very low mixing ratios at the top of the NBL, consequently leading to longer NO<sub>3</sub> lifetimes aloft. The reaction with various VOCs (R4), which are also emitted at the ground, could contribute to the fast NO<sub>3</sub> loss at the surface as well. The short NO<sub>3</sub> lifetime in the lower NBL, to a large extent, determined the low NO<sub>3</sub> mixing ratios even when a higher NO<sub>3</sub> production rate than aloft was present. Although aerosol uptake of N<sub>2</sub>O<sub>5</sub> (R6) following the equilibrium (R5) is an indirect NO<sub>3</sub> loss, as will be further discussed below, the extremely low RH (Fig. 8) minimizes the influence of (R6) on the NO<sub>3</sub> distribution in Phoenix. In addition, a temperature inversion in the stable NBL (Fig. 8) affects the height profile of the reaction rates of (R5) due to the strong temperature dependence of the equilibrium between reactants and the product (Geyer and Stutz, 2004a). Higher temperatures at the top of the NBL can thus result in a considerable shift of the equilibrium to the direction of NO<sub>3</sub> and contributed to the strong positive NO<sub>3</sub> vertical gradient during the stable periods on 26 June–27 June.

During the weak stability period,  $\tau_{\text{NO}_3}$  was surprisingly low at all altitudes (Fig. 7). The highest  $\tau_{\text{NO}_3}$  was only about 1 min. As indicated by the high wind speed (Fig. 8) and the weak vertical profiles of measured trace gases (Fig. 7), the vertical mixing during this period was strong. Ground-level emitted NO<sub>3</sub> sink species were transported upward efficiently and resulted in a rapid loss of NO<sub>3</sub> at all measured altitudes. Consequently the very short  $\tau_{\text{NO}_3}$  explains the particularly low NO<sub>3</sub> levels during this period despite a fairly constant P<sub>NO<sub>3</sub></sub> throughout the night.

In summary, the comparison of the NO<sub>3</sub> production rate and lifetime reveals that the positive NO<sub>3</sub> vertical gradients in urban areas are a consequence of the NO<sub>3</sub> loss that is more efficient near the ground. Neither NO<sub>3</sub> mixing ratio nor its atmospheric lifetime in the NBL can be determined based on ground-level measurements alone. These results support earlier model studies (Aliwell and Jones, 1998; Geyer and Stutz, 2004a) and suggest that calculations from ground measurements of NO<sub>3</sub> can lead to underestimation of the nocturnal oxidizing capacity of the atmosphere.

#### 4.4 Vertical profiles of the reservoir species N<sub>2</sub>O<sub>5</sub>

The formation of N<sub>2</sub>O<sub>5</sub> and its thermal decay (R5) result in a temperature dependent equilibrium between N<sub>2</sub>O<sub>5</sub>, NO<sub>3</sub>, and NO<sub>2</sub>. Ideally, in the absence of other N<sub>2</sub>O<sub>5</sub> sinks (i.e., R6), the chemical steady state N<sub>2</sub>O<sub>5</sub> concentration is determined by  $K_{\text{eq}}(T) \cdot [\text{NO}_2] \cdot [\text{NO}_3]$ , in which

$K_{\text{eq}}(T) = 5.5 \times 10^{-27} e^{10724/T} \text{cm}^3$  (Wangberg et al., 1997). Due to the very low RH in Phoenix, the influence of (R6) on the steady state of N<sub>2</sub>O<sub>5</sub> is rather unimportant. Based on this temperature dependent equilibrium, unique vertical profiles of chemical steady state N<sub>2</sub>O<sub>5</sub> mixing ratios were derived with the measured data of NO<sub>2</sub> and NO<sub>3</sub> as well as the temperature profile (Fig. 7). The temperature measured on top of ADEQ was taken as the upper box temperature. The average temperature on top of ADEQ and Hilton was used as the middle box temperature.

During the stable periods on the night of 26 June–27 June, N<sub>2</sub>O<sub>5</sub> mixing ratios reached up to 350 ppt, while they were below ~100 ppt during the unstable period, mainly because of the difference in NO<sub>3</sub> concentrations for different periods (see Sect. 4.3). N<sub>2</sub>O<sub>5</sub> during the stable periods showed considerably higher levels in the middle box than in the upper box. This negative N<sub>2</sub>O<sub>5</sub> vertical gradient was not reported in any earlier studies except in model calculations of a special urban case with very high ambient temperature (Geyer and Stutz, 2004a). The N<sub>2</sub>O<sub>5</sub> profiles during the unstable period were weak and showed higher or equal N<sub>2</sub>O<sub>5</sub> levels aloft than in the middle box, which is in agreement with the model results of most other scenarios (Geyer and Stutz, 2004a).

Based on the temperature dependent equilibrium, N<sub>2</sub>O<sub>5</sub> vertical distribution is influenced by the opposite vertical distribution of NO<sub>2</sub> and NO<sub>3</sub> and the temperature profile. The maximum temperature inversion during this night (~2 K difference between top of Hilton and top of ADEQ) could lead to at most 12% decrease in N<sub>2</sub>O<sub>5</sub> mixing ratios from the middle box to the upper box. The vertical variations of N<sub>2</sub>O<sub>5</sub> during this night were, therefore, mainly caused by the opposite vertical distribution of NO<sub>2</sub> and NO<sub>3</sub>.

Using an assumption of linear NO<sub>2</sub> and NO<sub>3</sub> distributions similar to the one used in the discussion of P<sub>NO<sub>3</sub></sub>, the N<sub>2</sub>O<sub>5</sub> mixing ratio at altitude  $z$  can be expressed as  $K_{\text{eq}} \cdot ([\text{NO}_2]_{z0} + \frac{d[\text{NO}_2]}{dz} \cdot \Delta z) \cdot ([\text{NO}_3]_{z0} + \frac{d[\text{NO}_3]}{dz} \cdot \Delta z)$ . Neglecting the possible height dependence of  $K_{\text{eq}}(T)$ , one can derive the gradient of steady state N<sub>2</sub>O<sub>5</sub> mixing ratios at a specific altitude:

$$\begin{aligned} \frac{\partial [\text{N}_2\text{O}_5]}{\partial z} &\approx [\text{N}_2\text{O}_5]_z \cdot \left( \frac{\frac{d[\text{NO}_3]}{dz}}{[\text{NO}_3]_z} + \frac{\frac{d[\text{NO}_2]}{dz}}{[\text{NO}_2]_z} \right) \\ &= [\text{N}_2\text{O}_5]_z \cdot (A - B) \end{aligned} \quad (7)$$

The sign of N<sub>2</sub>O<sub>5</sub> gradient is thus determined by the sum of the relative vertical gradients of NO<sub>3</sub>, A, and NO<sub>2</sub>, -B (note that the relative vertical gradient of NO<sub>2</sub> is always negative), at the corresponding altitude. For example, during the stable period on 26 June–27 June, a low NO<sub>2</sub> concentration and a strong vertical gradient of NO<sub>2</sub> could result in a large value of term B in Eq. (7) while term A was relatively small due to the high NO<sub>3</sub> concentration. A negative N<sub>2</sub>O<sub>5</sub> vertical gradient was thus determined. The high N<sub>2</sub>O<sub>5</sub> concentrations during this period further magnified this negative gradient (Eq. 7).

In contrast, term B in Eq. (7) during the unstable period was much smaller as a result of higher NO<sub>2</sub> levels and weaker vertical gradients, while term A became relatively large due to the very low NO<sub>3</sub> levels. The resulting positive N<sub>2</sub>O<sub>5</sub> vertical gradient was weak because of the low concentrations of N<sub>2</sub>O<sub>5</sub> during these hours.

It should be noted that the vertical transport of N<sub>2</sub>O<sub>5</sub> could influence the above-discussed steady state of N<sub>2</sub>O<sub>5</sub> under some circumstances. The impact of transport on the calculated N<sub>2</sub>O<sub>5</sub> distribution in Phoenix will be further investigated in a forthcoming paper using a 1-D chemical transport model.

Our studies show complex N<sub>2</sub>O<sub>5</sub> vertical profiles in the NBL depending on a number of factors. Although the role of the aerosol uptake of N<sub>2</sub>O<sub>5</sub> through (R6) is weakened in Phoenix due to the low RH, it can be an important atmospheric denoxification process which removes NO<sub>3</sub> and NO<sub>2</sub> and further an indirect loss of O<sub>3</sub> in other polluted areas with high RH and aerosol density. The N<sub>2</sub>O<sub>5</sub> profile, together with the vertical distribution of aerosols, can thus play an important role in determining the altitude dependence of the NBL O<sub>x</sub> sink in those cases.

#### 4.5 Budgets of O<sub>3</sub>, NO<sub>2</sub>, and O<sub>x</sub> in the NBL

As discussed in Sect. 4.1, nocturnal chemistry can influence O<sub>3</sub> levels for the following morning in polluted urban areas through its influence on the levels of total O<sub>x</sub> (see Eq. 3). The nocturnal budgets of both O<sub>3</sub> and NO<sub>2</sub> thus play critical roles.

The dominant O<sub>3</sub> loss during night-time is the reaction of O<sub>3</sub> with freshly emitted NO (R1). The true influence of this reaction on the O<sub>3</sub> levels for the following morning is the shift in the Leighton ratio (see Eqs. 1–2 in Sect. 4.1). The other important loss processes of O<sub>3</sub> in the NBL include its reaction with NO<sub>2</sub> (R2) and its heterogeneous destruction, either on aerosols,  $L_{O_3+aerosol}$ , or the ground,  $L_{O_3\text{ dry dep}}$ . Dry deposition of O<sub>3</sub> becomes particularly important in the case of low NO emissions (Sect. 4.2.3), but is negligible in heavily polluted areas where O<sub>3</sub> is already depleted at the ground (Sect. 4.2.2). In addition, the downward transport of O<sub>3</sub> from higher altitudes,  $VT_{O_3}$ , constitutes the only source of O<sub>3</sub> into the NBL. We can thus summarize the budget of O<sub>3</sub> in the NBL as:

$$\frac{d[O_3]}{dt} = -k_1 \cdot [O_3] \cdot [NO] - k_2 \cdot [O_3] \cdot [NO_2] - L_{O_3+aerosol} - L_{O_3\text{ dry dep}} + VT_{O_3} \quad (8)$$

The main source of NO<sub>2</sub> in the urban NBL is its formation through (R1). Due to the low NO<sub>2</sub>/NO<sub>x</sub> emission ratio, NO<sub>2</sub> direct emission,  $E_{NO_2}$ , generally plays a small role even when nocturnal emissions are particularly strong (for example, the case in Sect. 4.2.2). The formation of NO<sub>3</sub> (R2) is an NO<sub>2</sub> sink, while the loss of NO<sub>3</sub> through reaction with NO (R3) is another source of NO<sub>2</sub>. The N<sub>2</sub>O<sub>5</sub> chemistry is also

both a source and a sink of NO<sub>2</sub>. Thus the shift of the equilibrium of (R5) gives a measure of the impact of N<sub>2</sub>O<sub>5</sub> on the nocturnal NO<sub>2</sub> budget. Direct heterogeneous uptake of NO<sub>2</sub> on aerosols,  $L_{NO_2+aerosol}$ , and dry deposition on the ground,  $L_{NO_2\text{ dry dep}}$ , can also play a role. Finally the NBL NO<sub>2</sub> is lost by the upward transport to higher altitudes,  $VT_{NO_2}$ . The budget of NO<sub>2</sub> in the NBL is therefore given as:

$$\begin{aligned} \frac{d[NO_2]}{dt} = & k_1 \cdot [O_3] \cdot [NO] - k_2 \cdot [O_3] \cdot [NO_2] \\ & + 2k_3 \cdot [NO_3] \cdot [NO] \\ & + (k_{5-} \cdot [N_2O_5] - k_{5+} \cdot [NO_3] \cdot [NO_2]) \\ & - L_{NO_2+aerosol} - L_{NO_2\text{ dry dep}} + E_{NO_2} - VT_{NO_2} \quad (9) \end{aligned}$$

Based on these considerations, one can set up an expression for the total O<sub>x</sub> change in the NBL.

$$\begin{aligned} \frac{d[O_x]}{dt} = & -2 \cdot (k_2 \cdot [O_3] \cdot [NO_2] - k_3 \cdot [NO_3] \cdot [NO]) \\ & + (k_{5-} \cdot [N_2O_5] - k_{5+} \cdot [NO_3] \cdot [NO_2]) \\ & - L_{O_3+aerosol} - L_{O_3\text{ dry dep}} - L_{NO_2+aerosol} \\ & - L_{NO_2\text{ dry dep}} + E_{NO_2} + VT_{O_3} - VT_{NO_2} \quad (10) \end{aligned}$$

Assuming a chemical steady state of NO<sub>3</sub>, the terms in the first parenthesis in Eq. (10) describe the net NO<sub>3</sub> loss that does not regenerate O<sub>x</sub> (i.e., NO<sub>3</sub> loss through (R4) and the disequilibrium of (R5) as discussed in Sect. 4.1). Therefore, these terms can be replaced by  $L_{NO_3+VOC}$  and  $(k_{5+} \cdot [NO_3] \cdot [NO_2] - k_{5-} \cdot [N_2O_5])$ . Considering a steady state assumption for N<sub>2</sub>O<sub>5</sub>, the latter is equivalent to the heterogeneous uptake and the vertical transport of N<sub>2</sub>O<sub>5</sub>. Assuming that N<sub>2</sub>O<sub>5</sub> vertical transport only redistributes N<sub>2</sub>O<sub>5</sub> but does not influence the total N<sub>2</sub>O<sub>5</sub> budget in the NBL, the disequilibrium term,  $(k_{5+} \cdot [NO_3] \cdot [NO_2] - k_{5-} \cdot [N_2O_5])$ , is approximately equal to  $L_{N_2O_5+aerosol}$ .

For typical urban cases, Eq. (10) can be further simplified. Earlier studies show small influence of the aerosol uptake of both O<sub>3</sub> and NO<sub>2</sub> on the urban nocturnal budget of these species (Geyer and Stutz, 2004a). Considering the fact that dry deposition is determined by the ground level concentration of a species, the vertical exchange coefficient, and the reactive uptake coefficient, the dry deposition terms in Eq. (10) can be combined into  $L_{O_x\text{ dry dep}}$  assuming similar uptake coefficients of these two species. Vertical transport is an important loss and source of NBL NO<sub>2</sub> and O<sub>3</sub>, respectively. Since the vertical gradients of O<sub>3</sub> and NO<sub>2</sub> are often of the same magnitude but opposite signs (see Sects. 3 and 4.2), the O<sub>x</sub> loss due to the upward transport of NO<sub>2</sub> out of the NBL is as much as the O<sub>x</sub> source through the downward transport of O<sub>3</sub> into the NBL (i.e.,  $VT_{NO_2} = VT_{O_3}$ ). The two terms in Eq. (10),  $VT_{O_3} - VT_{NO_2}$ , therefore cancel out. This also implies that vertical transport can be an important NO<sub>2</sub> source in the RL and influences the chemistry at higher altitudes.

Following these arguments, one can conclude that the budget of O<sub>x</sub> in the NBL is dominated by the atmospheric

denoxification processes (i.e.,  $L_{N_2O_5+aerosol}$  and  $L_{NO_3+VOC}$ ), the dry deposition of O<sub>x</sub>, and the direct emission of NO<sub>2</sub>:

$$\frac{d[O_x]}{dt} = -3 \cdot L_{N_2O_5+aerosol} - 2 \cdot L_{NO_3+VOC} - L_{O_x \text{ dry dep}} + E_{NO_2} \quad (11)$$

It should be noted that the influence of N<sub>2</sub>O<sub>5</sub> aerosol uptake ( $L_{N_2O_5+aerosol}$ ), which is relatively unimportant for the chemical steady state of N<sub>2</sub>O<sub>5</sub> in the dry atmosphere of Phoenix, is tripled in the total O<sub>x</sub> loss rate and becomes an effective factor influencing the nocturnal budget of O<sub>x</sub>.

We can now apply these theoretical considerations to the observations in Phoenix. To derive a picture averaged for the entire NBL, the original measurement results along the lower light path spanning 140–10 m altitudes, which are approximately equivalent to the integrated trace gas concentrations in the lowest 140 m of the atmosphere, are used for discussing the NBL O<sub>x</sub> budget. We again use the nights discussed in Sect. 4.2, 16 June–17 June, 28 June–29 June, and 30 June–1 July, to show the influence of atmospheric stability and emissions on the total O<sub>x</sub> budgets. A linear fit of the change of O<sub>x</sub> concentrations along the lower light path from 20:00 (21:30 for the night of 16 June–17 June) until 04:00 was applied to determine the O<sub>x</sub> loss rate averaged throughout the night (Table 4). While this procedure works well with O<sub>x</sub>, it is less accurate for O<sub>3</sub> and NO<sub>2</sub> due to temporal variations. Figures 9 and 10 show large temporal variations of both NO<sub>2</sub> and O<sub>3</sub> levels during the night of 16 June–17 June and 28 June–29 June. The average rates of NO<sub>2</sub> and O<sub>3</sub> are thus difficult to estimate. Nevertheless, a linear fit was applied to get the O<sub>3</sub> and NO<sub>2</sub> change rates for the night of 30 June–1 July, during which the temporal variations are relatively weak (Fig. 11). The results in Table 4 show the comparison of the O<sub>x</sub> loss rates during the three nights investigated here. Considering the magnitude of the error bars and the temporal variations, the difference in the total O<sub>x</sub> loss during these nights is very small, despite the large difference in the meteorology and chemical conditions among these cases.

To understand this behavior, the factors determining the O<sub>x</sub> budget in Eq. (11) have to be investigated separately. (1) Denoxification processes: The significance of denoxification strongly depends on the levels of N<sub>2</sub>O<sub>5</sub> and NO<sub>3</sub>. High NO<sub>2</sub> and O<sub>3</sub> levels lead to high production rate of NO<sub>3</sub> and thus N<sub>2</sub>O<sub>5</sub>. For example, the highest NO<sub>3</sub> levels in this two-week experiment were observed during the night of 16 June–17 June with the strongest emissions (see Sect. 3.2). Figure 3 also shows higher NO<sub>3</sub> and NO<sub>2</sub> on 16 June–17 June than those on 30 June–1 July, suggesting higher steady-state N<sub>2</sub>O<sub>5</sub> levels on 16 June–17 June. The loss of O<sub>x</sub> through denoxification is therefore larger in the first case. (2) Dry deposition: The significance of dry deposition is more difficult to estimate since it depends on both O<sub>x</sub> levels and the vertical stability in the NBL. The O<sub>3</sub> deposition rate strongly decreases with the increase of surface NO emissions and the

increase of vertical stability. The O<sub>3</sub> dry deposition during the night of 16 June–17 June is thus much smaller than during the other night since both stability and emission strengths are in favor of a smaller O<sub>3</sub> deposition rate, especially during the later part of this night when O<sub>3</sub> was depleted. Dry deposition of NO<sub>2</sub> is, however, only weakly dependent on the NBL stability because the effects of reduced NO<sub>2</sub> levels near the ground and faster transport toward the surface due to a better mixing balance each other (Geyer and Stutz, 2004a). The NO emission rate has a strong influence on the NO<sub>2</sub> deposition and thus leads to a larger  $L_{NO_2 \text{ dry dep}}$  for the high emission night. The O<sub>3</sub> and NO<sub>2</sub> deposition rates thus change in different directions. The direct comparison of total O<sub>x</sub> deposition rates during these two nights cannot be made due to limited data of the stability and emission rates. (3) Direct emission: Finally, the influence of direct NO<sub>2</sub> emissions is obviously stronger when surface NO<sub>x</sub> emissions are higher (i.e., on the night of 16 June–17 June).

Based on these discussions, it can be concluded that the evaluation of O<sub>x</sub> loss in the NBL requires considerations of all the terms determining the nocturnal O<sub>x</sub> budget and thus can be very complex. The dry deposition term is especially difficult to evaluate and the contribution of O<sub>3</sub> and NO<sub>2</sub> needs to be treated separately for different conditions. Since the values of this term in urban scenarios modeled by Geyer and Stutz (2004a) are in the same order of magnitude as the average night-time O<sub>x</sub> loss rate in our observations, dry deposition plays an important role in the behavior of total O<sub>x</sub> change during these nights. It can be deduced that the combination of a larger loss rate by denoxification, a larger source rate by direction emission, and a most likely smaller O<sub>x</sub> deposition rate during 16 June–17 June results in a similar total O<sub>x</sub> loss rate for this night to that on 30 June–1 July.

It is interesting to note that the average O<sub>3</sub> loss rate during the night of 30 June–1 July was very close to the total O<sub>x</sub> loss rate. NO<sub>2</sub> levels did not show clear change throughout the night. A considerable NO<sub>2</sub> loss rate through vertical transport as a result of a weak stability most likely balanced the small NO<sub>2</sub> source rate due to the low nocturnal emissions. Therefore the influence of NBL chemistry on morning BL O<sub>3</sub> levels for this case is mostly the result of the nocturnal O<sub>x</sub> loss. The influence caused by nocturnal emissions through the shift of Leighton Ratio (see Eq. 2 in Sect. 4.1) is negligible. This conclusion can be further confirmed by the calculation of the ultimate O<sub>3</sub> loss as a result of the total O<sub>x</sub> loss and the change of NO<sub>x</sub> for this night (Table 5). Based on the interpretation of linear fit results discussed in Table 4, the O<sub>x</sub> and NO<sub>2</sub> levels at about 19:30 (right before sunset) and 05:30 (right after sunrise) are estimated. The corresponding NO levels are evaluated based on in situ measurements. Therefore, without the impact of any other factors such as early morning convections, the total O<sub>x</sub> and total NO<sub>x</sub> change in the NBL are estimated to be -26 ppb and 2 ppb, respectively. Using Eq. (1) and the estimated O<sub>x</sub> and NO<sub>x</sub> levels, O<sub>3</sub> mixing ratios right before sunset and right

**Table 5.** Evaluation of the ultimate O<sub>3</sub> loss during the night of 30 June–1 July.

	[O <sub>x</sub> ] from interpreted DOAS data	[NO <sub>2</sub> ] from interpreted DOAS data	[NO] from in situ data	[O <sub>3</sub> ] from Eq. (1)
19:30	48 ppb	16 ppb	1 ppb	31 ppb
05:30	22 ppb	14 ppb	5 ppb	4 ppb
	Δ[O <sub>x</sub> ]	Δ[NO <sub>x</sub> ]		Δ[O <sub>3</sub> ]
19:30–05:30	–26 ppb	2 ppb		–27 ppb

after sunrise are calculated to be 31 ppb and 4 ppb, giving a 27 ppb ultimate reduction of the O<sub>3</sub> level. Assuming a constant NO<sub>x</sub> level, one can derive the ultimate O<sub>3</sub> loss caused by only O<sub>x</sub> loss through nocturnal chemistry to be 25 ppb, which contributes 92% to the ultimate O<sub>3</sub> loss. The influence of nocturnal emissions (i.e., the increase of total NO<sub>x</sub> levels) is rather small (~2 ppb) for this weakly polluted case.

In contrast, during the heavily polluted night of 16 June–17 June, the nocturnal O<sub>x</sub> loss is relatively smaller and thus contributed less to the ultimate O<sub>3</sub> removal. NO<sub>x</sub> levels could increase considerably as a result of the strong NO emission followed by (R1) and the direct emission of NO<sub>2</sub>. The strong NBL stability that led to ineffective upward transport of NO<sub>x</sub> out of the NBL could also contribute to the NO<sub>x</sub> increase by reducing the NO<sub>x</sub> loss term. Consequently, the contribution of the shift of Leighton Ratio (see Eq. 2) to the ultimate O<sub>3</sub> loss is more significant for this heavily polluted case. Unfortunately a quantitative evaluation is not possible for this night as a result of the temporal variations in NO<sub>2</sub> and O<sub>3</sub> levels and the missing data in the early evening.

The comparison of O<sub>x</sub> loss for these different cases suggests that the influence of nocturnal chemistry on O<sub>3</sub> levels in the next morning by changing total O<sub>x</sub> levels in the NBL (see Eq. 3) can be similar in cases with different emissions and stability. The nocturnal NO emission followed by (R1), which only redistribute NO<sub>2</sub> and O<sub>3</sub> without changing total O<sub>x</sub> and influence the morning O<sub>3</sub> levels through its influence on the Leighton Ratio, is however more important in heavily polluted areas (see Eq. 2).

## 5 Conclusions

Strong positive vertical gradients of O<sub>3</sub> and NO<sub>3</sub> and negative vertical gradients of NO<sub>2</sub>, HONO and HCHO in the stable NBL were observed in the downtown area of Phoenix. The magnitudes of the gradients were significantly larger than in various earlier observations in rural or suburban areas due to the higher night-time ground-level emissions. The major features of the measured profiles are consistent with the concept of the night-time trapping of local pollutants in a stable NBL. The details of the interaction of processes involved in this chemistry system with vertical transport are,

however, complex, depending on many factors. The following conclusions were drawn from our observations.

- The distinctive vertical distributions of reactive species compose a complex height-dependent nocturnal chemical system. Consequently, the atmospheric lifetimes of reactive species, the oxidative capacity of the NBL, the atmospheric denoxification process, and the O<sub>3</sub> production potential in the early morning boundary layer are strongly height-dependent.
- Vertical stability has a strong influence on the distribution of all trace gases in urban environments. Fast changes in vertical stability, as shown by the change in temperature gradients during the night and the onset of vertical mixing in the morning were observed to redistribute trace gases throughout the boundary layer.
- NO titration, as shown by the vertical profiles of NO<sub>2</sub>, O<sub>3</sub> and O<sub>x</sub>, plays a dominant role for the chemistry in the NBL. The surface emission strength of NO is a critical factor governing the magnitude and the shape of the vertical profiles.
- Vertical profiles of NO<sub>3</sub>, are predominately caused by the short steady-state lifetime of NO<sub>3</sub> at the ground as a result of the fast reactions with ground-level emitted NO. NO<sub>3</sub> production rates, which demonstrated complicated vertical profiles depending on the distribution of both NO<sub>2</sub> and O<sub>3</sub>, have a weaker influence.
- Calculated steady state N<sub>2</sub>O<sub>5</sub> concentration showed unique vertical profiles, which are a function of the ambient temperature and the distribution of NO<sub>2</sub> and NO<sub>3</sub>. These vertical profiles, together with possible aerosol profiles, lead to vertical variations of the aerosol uptake of N<sub>2</sub>O<sub>5</sub>, an indirect NO<sub>3</sub> loss and an important atmospheric denoxification process.
- O<sub>x</sub> levels decreased gradually throughout all nights. The removal of O<sub>x</sub> proceeds mainly through denoxification (i.e., NO<sub>3</sub>+VOC reactions and N<sub>2</sub>O<sub>5</sub> uptake) and dry deposition. Dry deposition on the ground is often not important in strongly polluted urban cases due to the low ground level O<sub>3</sub>. However, elevated NO<sub>2</sub> levels in

these cases lead to larger NO<sub>2</sub> deposition. The total nocturnal O<sub>x</sub> loss was observed to be of similar magnitude during nights with different emission strength, which is believed to be the result of the balance between a decreased dry deposition loss and an increased O<sub>x</sub> source (i.e., direct NO<sub>2</sub> emissions) as the surface emissions increase.

- Ozone loss in the NBL proceeds through the loss of O<sub>x</sub> and the impact of nocturnal NO emissions on the photo-stationary state in the morning. The latter is expected to be relatively more important in heavily polluted urban areas. It should be noted that this conclusion does not consider the influence of elevated NO<sub>x</sub> on photochemical ozone formation that starts a few hours after sunrise.

These vertical variations of nocturnal chemistry, especially for urban cases with strong surface emissions, are often not considered well in many atmospheric chemistry field experiments or current air quality modeling studies. The results of our observations show strong impact of these variations on the morning chemistry and suggest that vertically highly resolved chemical-transport models, which include the quantitative determination of vertical transport of various trace gases, are necessary to accurately describe the budgets of O<sub>3</sub>, NO<sub>2</sub>, and many other trace gases in the stable NBL.

*Acknowledgements.* We gratefully acknowledge the support of the Department of Energy, grant DE-FG03-01ER63094 and the atmospheric chemistry program of the National Science Foundation, award ATM-0348674. The assistance of Arizona Department of Environmental Quality is greatly appreciated. We would also like to thank C. W. Spicer from Battelle Columbus Operations for the in-situ measurements on BankOne, J. D. Fast and C. C. Doran from Pacific Northwest National Laboratory for providing meteorological data, C. Berkowitz, and R. Redman for their help in establishing the measurement site.

Edited by: A. Richter

## References

- Abram, J. P., Creasey, D. J., Heard, D. E., Lee, J. D., and Pilling, M. J.: Hydroxyl radical and ozone measurements in England during the solar eclipse of 11 August 1999, *Geophys. Res. Lett.*, **27**, 3437–3440, 2000.
- Alicke, B., Platt, U., and Stutz, J.: Impact of nitrous acid photolysis on the total hydroxyl radical budget during the LOOP/PIPPO study in Milan, *J. Geophys. Res.*, **107**, 8196, 2002.
- Aliwell, S. R. and Jones, R. L.: Measurements of tropospheric NO<sub>3</sub> at midlatitude, *J. Geophys. Res.*, **103**, 5719–5727, 1998.
- Aneja, V. P., Mathur, R., Arya, S. P., Li, Y., Murray, G. C., and Manuszak, T. L.: Coupling the vertical distribution of ozone in the atmospheric boundary layer, *Environ. Sci. Technol.*, **34**, 2324–2329, 2000.
- Atkinson, R., Baulch, D. L., Cox, R. A., Crowley, J. N., Hampson, R. F., Hynes, R. G., Jenkin, M. E., Rossi, M. J., and Troe, J.: Evaluated kinetic and photochemical data for atmospheric chemistry: Volume I – gas phase reactions of O<sub>x</sub>, HO<sub>x</sub>, NO<sub>x</sub> and SO<sub>x</sub> species, *Atmos. Chem. Phys.*, **4**, 1461–1738, 2004, <http://www.atmos-chem-phys.net/4/1461/2004/>.
- Aumont, B., Chervier, F., and Laval, S.: Contribution of HONO sources to the NO<sub>x</sub>/HO<sub>x</sub>/O<sub>3</sub> chemistry in the polluted boundary layer, *Atmos. Environ.*, **37**, 487–498, 2003.
- Brown, S. S., Stark, H., and Ravishankara, A. R.: Applicability of the steady state approximation to the interpretation of atmospheric observations of NO<sub>3</sub> and N<sub>2</sub>O<sub>5</sub>, *J. Geophys. Res.*, **108**, 4539–4548, 2003.
- Chen, C., Tsuang, B., Tu, C., Cheng, W., and Lin, M.: Wintertime vertical profiles of air pollutants over a suburban area in central Taiwan, *Atmos. Environ.*, **36**, 2049–2059, 2002.
- Colbeck, I. and Harrison, R. M.: Dry deposition of ozone: some measurements of deposition velocity and of vertical profiles to 100 meters, *Atmos. Environ.*, **19**, 1807–1818, 1985.
- Cros, B., Fontan, J., Minga, A., Helas, G., Nganga, D., Delmas, R., Chapuis, A., Benech, B., Druihel, A., and Andreae, M. O.: Vertical profiles of ozone between 0 meters and 400 meters in and above the African Equatorial Forest, *J. Geophys. Res.*, **97**, 12 877–12 887, 1992.
- Dentener, F. J. and Crutzen, P. J.: Reaction of N<sub>2</sub>O<sub>5</sub> on tropospheric aerosols: Impact on the global distributions of NO<sub>x</sub>, O<sub>3</sub>, and OH, *J. Geophys. Res.*, **98**, 7149–7163, 1993.
- Doran, J. C., Berkowitz, C. M., Coulter, R. L., Shaw, W. J., and Spicer, C. W.: The 2001 Phoenix Sunrise Experiment: vertical mixing and chemistry during the morning transition in Phoenix, *Atmos. Environ.*, **37**, 2365–2377, 2003.
- Fast, J. D., Doran, J. C., Shaw, W. J., Coulter, R. L., and Martin, T. J.: The evolution of the boundary layer and its effect on air chemistry in the Phoenix area., *J. Geophys. Res.*, **105**, 22 833–22 848, 2000.
- Fast, J. D., Torcolini, J. C., and Redman, R.: Pseudovertical temperature profiles and the urban heat island measured by a temperature datalogger network in Phoenix, Arizona, *J. Appl. Meteorol.*, **44**, 3–13, 2005.
- Finlayson-Pitts, B. J. and Pitts, J. N.: Chemistry of the upper and lower atmosphere: theory, experiments and applications, Academic Press, San Diego; London, 2000.
- Finlayson-Pitts, B. J., Wingen, L. M., Sumner, A. L., Syomin, D., and Ramazan, K. A.: The heterogeneous hydrolysis of NO<sub>2</sub> in laboratory systems and in outdoor and indoor atmospheres: An integrated mechanism, *Phys. Chem. Chem. Phys.*, **5**(2), 223–242, 2003.
- Fish, D. J., Shallcross, D. E., and Jones, R. L.: The vertical distribution of NO<sub>3</sub> in the atmospheric boundary layer, *Atmos. Environ.*, **33**, 687–691, 1999.
- Friedeburg, C., Wagner, T., Geyer, A., Kaiser, N., Vogel, B., Vogel, H., and Platt, U.: Derivation of tropospheric NO<sub>3</sub> profiles using off-axis differential optical absorption spectroscopy measurements during sunrise and comparison with simulations, *J. Geophys. Res.*, **107**, 4168–4195, 2002.
- Galbally, I.: Some measurements of ozone variation and destruction in the atmospheric surface layer, *Nature*, **218**, 456–457, 1968.
- Garland, J. A. and Branson, J. R.: The mixing height and mass balance of SO<sub>2</sub> in the atmosphere above Great Britain, *Atmos. Environ.*, **10**, 353–362, 1976.
- Geyer, A., Alicke, B., Mihelcic, D., Stutz, J., and Platt, U.: Compar-

- ison of tropospheric NO<sub>3</sub> radical measurements by differential optical absorption spectroscopy and matrix isolation spin resonance, *J. Geophys. Res.*, 104, 26 097–26 105, 1999.
- Geyer, A. and Stutz, J.: Vertical profiles of NO<sub>3</sub>, N<sub>2</sub>O<sub>5</sub>, O<sub>3</sub>, and NO<sub>x</sub> in the nocturnal boundary layer: 2. Model studies on the altitude dependence of composition and chemistry, *J. Geophys. Res.*, 109, D12 307, doi:10.1029/2003JD004211, 2004a.
- Geyer, A. and Stutz, J.: The vertical structure of OH-HO<sub>2</sub>-RO<sub>2</sub> chemistry in the nocturnal boundary layer: a one-dimensional model study, *J. Geophys. Res.*, 109, D16 301, doi:10.1029/2003JD004425, 2004b.
- Glaser, K., Vogt, U., and Baumbach, G.: Vertical profiles of O<sub>3</sub>, NO<sub>2</sub>, NO<sub>x</sub>, VOC, and meteorological parameters during the Berlin Ozone Experiment (BERLIOZ) campaign, *J. Geophys. Res.*, 108, 8253–8266, 2003.
- Gusten, H., Heinrich, G., and Sprung, D.: Nocturnal depletion of ozone in the upper Rhine Valley, *Atmos. Environ.*, 32, 1195–1202, 1998.
- Harrison, R. M., Holmann, C. D., McCartney, H. A., and McIlvern, J. F. R.: Nocturnal depletion of photochemical ozone at a rural site, *Atmos. Environ.*, 12, 2021–2026, 1978.
- Hov, O.: One-dimensional vertical model for ozone and other gases in the atmosphere boundary layer, *Atmos. Environ.*, 17, 535–550, 1983.
- Jenkin, M. E. and Clemmshaw, K. C.: Ozone and other secondary photochemical pollutants: chemical processes governing their formation in the planetary boundary layer, *Atmos. Environ.*, 34, 2499–2527, 2000.
- Kleinman, L., Lee, Y.-N., Springston, S. R., Nunnermacker, L., Zhou, X., Brown, R., Hallock, K., Klotz, P., Leahy, D., Lee, J. H., and Newman, L.: Ozone formation at a rural site in the southeastern United States, *J. Geophys. Res.*, 99, 3469–3482, 1994.
- Kurtenbach, R., Ackermann, R., Becker, K. H., Geyer, A., Gomes, J. A. G., Lorzer, J. C., Platt, U., and Wiesen, P.: Verification of the contribution of vehicular traffic to the total NMVOC emissions in Germany and the importance of the NO<sub>3</sub> chemistry in the city air, *J. Atmos. Chem.*, 42, 395–411, 2002.
- McKendry, I. G., Steyn, D. G., Lundgren, J., Hoff, R. M., Strapp, W., Anlauf, K., Froude, F., Martin, J. B., Banta, R. M., and Olivier, L. D.: Elevated ozone layers and vertical down-mixing over the lower Fraser Valley, BC, *Atmos. Environ.*, 31, 2135–2146, 1997.
- Meller, R. and Moortgart, G. K.: Temperature dependence of the absorption cross sections of formaldehyde between 223 and 323 K in the wavelength range 225–375 nm, *J. Geophys. Res.*, 201, 7089–7101, 2000.
- Neu, U., Kunzle, T., and Wanner, H.: On the relation between ozone storage in the residual layer and daily variation in near-surface ozone concentration – A case study, *Boundary Layer Meteorology*, 69, 221–247, 1994.
- Pisano, J. T., McKendry, I., Steyn, D. G., and Hastie, D. R.: Vertical nitrogen dioxide and ozone concentrations measured from a tethered balloon in the lower Fraser Valley, *Atmos. Environ.*, 31, 2071–2078, 1997.
- Sadanaga, Y., Matsumoto, J., and Kajji, Y.: Photochemical reactions in the urban air: Recent understandings of radical chemistry, *J. Photochem. Photobiol. C – Photochem. Rev.*, 4, 85–104, 2003.
- Sander, S. P.: Temperature dependence of the NO<sub>3</sub> absorption spectrum, *J. Phys. Chem.*, 90, 4135–4142, 1986.
- Smith, G. D., Molina, L. T., and Molina, M. J.: Measurement of radical quantum yields from formaldehyde photolysis between 269 and 339 nm, *J. Phys. Chem. A*, 106, 1233–1240, 2002.
- Stockwell, W. R., Kirchner, F., Kuhn, M., and Seefeld, S.: A new mechanism for regional atmospheric chemistry modeling, *J. Geophys. Res.*, 102, 25 847–25 879, 1997.
- Stutz, J. and Platt, U.: Numerical analysis and estimation of the statistical error of differential optical absorption spectroscopy measurements with least-squares methods, *Appl. Opt.*, 35(30), 6041–6053, 1996.
- Stutz, J., Kim, E. S., Platt, U., Bruno, P., Perrino, C., and Febo, A.: UV-visible absorption cross sections of nitrous acid, *J. Geophys. Res.*, 105, 14 585–14 592, 2000.
- Stutz, J., Alicke, B., and Neftel, A.: Nitrous acid formation in the urban atmosphere: Gradient measurements of NO<sub>2</sub> and HONO over grass in Milan, Italy, *J. Geophys. Res.*, 107, 8192–8207, 2002.
- Stutz, J., Alicke, B., Ackermann, R., Geyer, A., Wang, S., White, A. B., Williams, E. J., Spicer, C. W., and Fast, J. D.: Relative humidity dependence of HONO chemistry in urban areas, *J. Geophys. Res.*, 109, 3307–3318, 2004a.
- Stutz, J., Alicke, B., Ackermann, R., Geyer, A., White, A., and Williams, E.: Vertical profiles of NO<sub>3</sub>, N<sub>2</sub>O<sub>5</sub>, O<sub>3</sub>, and NO<sub>x</sub> in the nocturnal boundary layer: 1. Observations during the Texas Air Quality Study 2000, *J. Geophys. Res.*, 109, D12 306, doi:10.1029/2003JD004209, 2004b.
- Van Dop, H., Guicherit, R., and Lanting, R. W.: Some measurements of the vertical distribution of ozone in the atmospheric boundary layer, *Atmos. Environ.*, 11, 65–71, 1977.
- Voigt, S., Orphal, J., and Burrows, J. P.: The temperature and pressure dependence of the absorption cross-sections of NO<sub>2</sub> in the 250–800 nm region measured by Fourier-transform spectroscopy, *J. Photochem. Photobiol. A – Chem.*, 149, 1–7, 2002.
- Wangberg, I., Etkorn, T., Barnes, I., Platt, U., and Becker, K. H.: Absolute determination of the temperature behavior of the NO<sub>2</sub>+NO<sub>3</sub>+(M)↔N<sub>2</sub>O<sub>5</sub>+(M) equilibrium, *J. Phys. Chem. A*, 101, 9694–9698, 1997.
- Wesely, M. L. and Hicks, B. B.: A review of the current status of knowledge on dry deposition, *Atmos. Environ.*, 34, 2261–2282, 2000.
- Zhang, J. and Rao, S. T.: The role of vertical mixing in the temporal evolution of ground-level ozone concentrations, *J. Appl. Meteorol.*, 38, 1674–1691, 1999.